Investigating the Evolution of *Drosophila* STING-Dependent Antiviral Innate Immunity by Multispecies Comparison of 2′3′-cGAMP Responses

Léna Hédelin,[1,†] Antonin Thiébaut,[2,†] Jingxian Huang,[3] Xiaoyan Li,[3] Aurélie Lemoine,[1] Gabrielle Haas,[1] Carine Meignin,[1] Hua Cai,[3] Robert M. Waterhouse,[2,*] Nelson Martins,[1,4,*] and Jean-Luc Imler[1,3,*]

[1]CNRS UPR9022, Institut de Biologie Moléculaire et Cellulaire, Université de Strasbourg, Strasbourg, France

[2]Department of Ecology and Evolution, SIB Swiss Institute of Bioinformatics, University of Lausanne, Lausanne, Switzerland

[3]School of Basic Medical Science, Sino-French Hoffmann Institute, Guangzhou Medical University, Guangzhou, China

[4]Present address: Católica Biomedical Research Centre, Católica Medical School, Universidade Católica Portuguesa Lisbon, Portugal / Instituto Gulbenkian de Ciência, Oeiras, Portugal

[†]These authors contributed equally to this work.

***Corresponding authors**: E-mails: robert.waterhouse@gmail.com; nelson.e.v.martins@gmail.com; jl.imler@ibmc-cnrs.unistra.fr.

Associate editor: Harmit Malik

Abstract

Viruses represent a major threat to all animals, which defend themselves through induction of a large set of virus-stimulated genes that collectively control the infection. In vertebrates, these genes include interferons that play a critical role in the amplification of the response to infection. Virus- and interferon-stimulated genes include restriction factors targeting the different steps of the viral replication cycle, in addition to molecules associated with inflammation and adaptive immunity. Predictably, antiviral genes evolve dynamically in response to viral pressure. As a result, each animal has a unique arsenal of antiviral genes. Here, we exploit the capacity to experimentally activate the evolutionarily conserved stimulator of IFN genes (STING) signaling pathway by injection of the cyclic dinucleotide 2′3′-cyclic guanosine monophosphate-adenosine monophosphate into flies to define the repertoire of STING-regulated genes in 10 *Drosophila* species, spanning 40 million years of evolution. Our data reveal a set of conserved STING-regulated factors, including STING itself, a cGAS-like-receptor, the restriction factor pastel, and the antiviral protein Vago, but also 2 key components of the antiviral RNA interference pathway, Dicer-2, and Argonaute2. In addition, we identify unknown species- or lineage-specific genes that have not been previously associated with resistance to viruses. Our data provide insight into the core antiviral response in *Drosophila* flies and pave the way for the characterization of previously unknown antiviral effectors.

Key words: **cGAS/STING, evo-immuno, *Drosophila*, transcriptome, 2′3′-cGAMP.**

Introduction

Innate immunity is the first line of host-defense in animals once pathogens have breached epithelial barriers. In the context of viral infections, 2 major types of host responses have been described. The first mechanism, RNA interference (RNAi), relies on RNaseIII enzymes of the Dicer family, which sense double stranded (ds) RNA generated during viral replication and process them into small interfering (si) RNA duplexes of 20 to 25 base pairs (bp) (Bronkhorst and van Rij 2014; Aguiar et al. 2016; Guo et al. 2019). One strand of the duplex is then loaded onto RNaseH enzymes of the Argonaute (AGO) family and serves to guide them toward complementary RNA molecules for cleavage or inhibition. RNAi plays a key role in the control of viruses in plants and nematodes, in which endogenous cellular RNA-dependent RNA polymerases (RdRPs) can amplify the response and generate secondary siRNAs (Ratcliff et al. 1997; Hamilton and Baulcombe 1999; Lu et al. 2005). RNAi also contributes to antiviral immunity in insects and mammals (Galiana-Arnoux et al. 2006; van Rij et al. 2006; Wang et al. 2006; Adiliaghdam et al. 2020; Poirier et al. 2021). In the model insect *Drosophila melanogaster*, 1 of the 2 Dicers, Dicer-2, is dedicated to the processing of long dsRNAs and antiviral defenses (Galiana-Arnoux et al. 2006; Wang et al. 2006; Donelick et al. 2020) and the siRNAs produced are loaded onto the protein AGO2, which cleaves and silences viral RNAs (van Rij et al. 2006; Wang et al. 2006; Marques et al. 2013).

The second mechanism consists of induced transcriptional responses that mediate production of antiviral restriction factors and cytokines that orchestrate the organismal response to the infection. It relies on pattern recognition

Received: October 13, 2023. **Revised:** January 30, 2024. **Accepted:** February 07, 2024

Discoveries

Open Access

receptors (PRRs) that detect viral nucleic acids and trigger gene expression (Kawai and Akira 2011). In vertebrates, viral RNAs can be recognized by PRRs of the Toll-like-receptor family (TLR3, 7, 8) or the retinoic acid-inducible gene I (RIG-I)-like-receptor family (RIG-I, MDA5), while viral DNAs are sensed by TLR9, the inflammasome-activating protein Absent in Melanoma (AIM)2 or the enzyme cyclic guanosine monophosphate (GMP)-adenosine monophosphate (AMP) synthase (cGAS) (Roers et al. 2016; Dalskov et al. 2023). The latter synthesizes the cyclic dinucleotide (CDN) 2′3′-cyclic GMP-AMP (cGAMP), which acts as a second messenger and binds to the protein stimulator of IFN genes (STING) in the membranes of the endoplasmic reticulum to activate signaling leading to gene induction (reviewed in Ablasser and Chen (2019)). Inducible antiviral responses are predominant in vertebrates, where the induced genes include those encoding type I and III interferons (IFN) (Dalskov et al. 2023). These cytokines amplify the antiviral response by upregulating hundreds of interferon stimulated genes (ISGs), the products of which work together to control viral infection (Schneider et al. 2014). Examples of well characterized products of ISGs include protein kinase R (PKR), an eIF2α kinase that blocks translation initiation (Williams 1999), IFN-induced protein with tetratricopeptide repeats (IFIT)1, which binds to and inhibits viral mRNAs lacking 2′-O methylation (Daffis et al. 2010; Pichlmair et al. 2011), and viperin, which synthesizes the antiviral chain terminator ribonucleotide 3′-deoxy-3′,4′-didehydrocytidine triphosphate (ddhCTP) (Gizzi et al. 2018).

Modifications of the transcriptome upon viral infections were also described in *Drosophila* and other insects, but it was not clear if they represented *bona fide* immune responses or reactions to the stress of the infection (e.g. cell lysis and release of cellular debris) (Dostert et al. 2005; Deddouche et al. 2008; Souza-Neto et al. 2009; Xu et al. 2012; Kemp et al. 2013; Panda et al. 2014; Sansone et al. 2015; Merkling et al. 2015a; Merkling et al. 2015b; Lamiable et al. 2016; Gordon et al. 2018; Swevers et al. 2018; Segrist et al. 2021). However, the discovery of IFN-like induced responses in oysters and sea anemones, as well as the genetic characterization of the contribution of an induced intracellular pathogen response in the nematode *Caenorhabditis elegans* have recently highlighted the importance of transcriptional responses to the control of viral infections in invertebrates (Lafont et al. 2020; Lewandowska et al. 2021; Margolis et al. 2021; Lažetić et al. 2023; Li et al. 2023). In addition, the recent description of STING-dependent induced antiviral responses in *D. melanogaster* and the silkworm *Bombyx mori* paved the way for the genetic characterization of a PRR-dependent antiviral pathway in insects (Goto et al. 2018; Hua et al. 2018). This pathway can be activated by 2 cGAS-like-receptors (cGLR1 and −2), which can bind dsRNA in virus-infected cells and produce cyclic dinucleotides (CDNs), including 2′3′-cGAMP, that act as second messengers (Hua et al. 2018; Cai et al. 2020; Holleufer et al. 2021; Slavik et al. 2021; Cai et al. 2023). Engagement of STING by CDNs triggers signaling that leads to activation of Relish, 1 of the 3 nuclear factor-κB family members in *Drosophila*, and induction of genes associated with antiviral immunity (Goto et al. 2018; Cai et al. 2020; Segrist et al. 2021).

Besides PKR, viperin, and other vertebrate antiviral effectors mentioned above, many ISGs remain poorly studied, although their protein products represent interesting candidates for new antiviral restriction factors (Schoggins et al. 2011, 2014; Schoggins 2019). Indeed, elucidating the mechanism of action of antiviral molecules has the potential to reveal weak spots in a virus or a family of viruses. Understandably, studies on ISGs have until recently largely relied on humans and the mouse model. One caveat of this approach is that it overlooks biodiversity and the fact that during the never-ending arms race between hosts and viruses, diversification of the portfolio of antiviral defenses is expected to occur in the hosts (Daugherty and Malik 2012; Goodin et al. 2016; McDougal et al. 2022). When it comes to biodiversity, insects with their 1.2 million known species are unmatched, offering the opportunity to extend the repertoire of antiviral genes (Jactel et al. 2021; Imler et al. 2024).

The discovery that injection of CDNs into flies induces a potent transcriptional response associated with antiviral protection provides a powerful means to identify antiviral genes in *Drosophila*, without the caveat of the stress reactions triggered by cell lysis or tissue damage associated with viral infection. This paves the way for evolutionary immunology studies aimed at comparing the repertoire of antiviral genes in different species (Imler et al. 2024). Here, we exploit the CDN STING-agonist injection assay to explore the evolution of STING-dependent antiviral immunity in 10 different *Drosophila* species.

Results

Virus- and Phylogeny-dependent Sensitivity to *Dicistroviridae* Infections

We selected 10 *Drosophila* species to investigate the evolution of STING-dependent responses. These species shared their last common ancestor 25 to 40 million years ago (Obbard et al. 2012) and include closely related species (e.g. *D. sechellia* and *D. simulans*; *D. santomea* and *D. yakuba* within the Sophophora subgenus) and very distantly related species (e.g. *D. mojavensis* and *D. virilis* in the Drosophila subgenus). These flies differ in their geographic distributions with some of them being cosmopolitan, continental, or restricted to islands. Accordingly, these species vary in their ecologies such as their diets, which are expected to expose them to different pathogens (Fig. 1).

We first investigated the sensitivity of adult flies from the different species to *Drosophila* C Virus (DCV), a natural pathogen of *D. melanogaster* which is a strong inducer of the STING pathway (Dostert et al. 2005; Goto et al. 2018; Liu et al. 2018; Holleufer et al. 2021). We injected male adult flies of each species with Tris buffer or DCV and monitored survival over 20 d (supplementary fig. S1a, Supplementary Material online). In parallel we measured

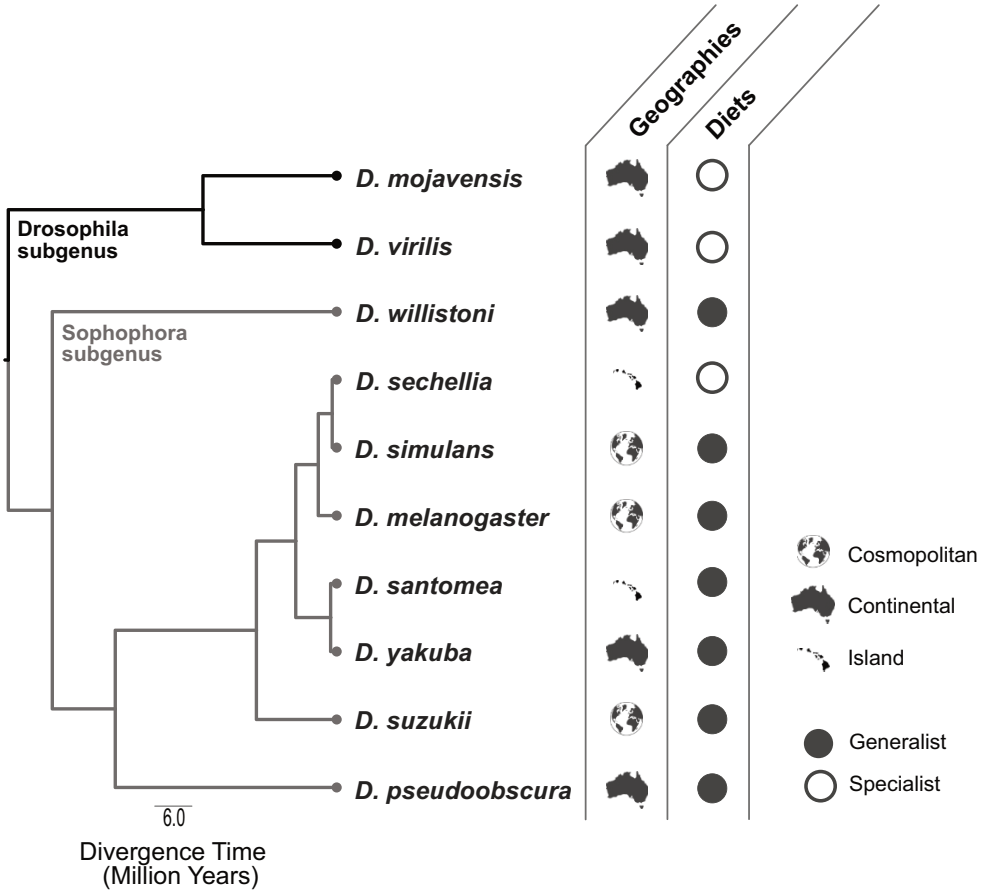

Fig. 1. Rationale for the selection of the 10 *Drosophila* species. Phylogeny based on Thiébaut et al. (2023) reconstruction. *Drosophila* species are separated into the Drosophila (black) and Sophophora (gray) subgenera. Approximate geographical range and food specialization are indicated.

viral RNA loads 2- and 3-days post infection (supplementary fig. S1b, Supplementary Material online). Three broad categories of species can be observed: some species like *D. melanogaster*, *D. simulans*, and *D. pseudoobscura* (species in group A in supplementary fig. S1a, Supplementary Material online) show high mortality after infection, whilst others resist infection by DCV (e.g. *D. santomea*, *D. yakuba*, *D. suzukii*, *D. virilis*, and *D. mojavensis*, species in group F in supplementary fig. S1a, Supplementary Material online). The third category, which includes *D. sechellia* and *D. willistoni*, shows an intermediate response (Fig. 2). The results are overall in line with a previous study that investigated the susceptibility of 48 species of Drosophilidae to DCV infection (Longdon et al. 2015), although some differences can be noted (e.g. intermediate susceptibility of *D. melanogaster* to DCV in (Longdon et al. 2015)), which may reflect differences in genetic background or infection method. However, as previously noted (Longdon et al. 2015), sensitivity to DCV does not relate to the evolutionary distance to the discovery host, *D. melanogaster*, with distantly related species (e.g. *D. pseudoobscura*) having more similar susceptibility phenotypes than closely related ones (e.g *D. yakuba* or *D. santomea*) . DCV viral RNA loads highlighted 2 major categories of species, those poorly supporting DCV replication (*D. virilis* and *D. mojavensis*) and those in which substantial amounts of DCV RNA were detected 2- and 3-days post infection (supplementary fig. S1b, Supplementary Material online). Among the latter, we observe 2 categories of species, those bearing low to medium viral RNA loads (e.g. *D. santomea*, *D. yakuba*, *D. suzukii*, and *D. willistoni*) and those bearing high viral RNA loads (e.g. *D. melanogaster*, *D. simulans*, *D. sechellia*, and *D. pseudoobscura*). Overall, viral RNA loads are consistent with the observed mortality profiles after DCV infection (Fig. 2; supplementary fig. S2a, Supplementary Material online).

One caveat of the previous experiment is that DCV, as a natural pathogen of *D. melanogaster*, might introduce a co-evolution bias in our analysis. To circumvent this possibility, we repeated the experiment with another *Dicistroviridae*, Cricket Paralysis Virus (CrPV). CrPV was isolated from Australian field crickets and is known for its virulence in a broad range of insect hosts, including *Drosophila* (Plus et al. 1978; van Rij et al. 2006) (supplementary fig. S3, Supplementary Material online). Survival analysis showed 2 categories of species, low, or average susceptibility to CrPV (*D. simulans*, *D. sechellia*, and *D. yakuba*, groups C in supplementary fig. S2a, Supplementary Material online), and highly susceptible (Fig. 2). Of note, CrPV infection led to rapid death of *D. virilis* and *D. mojavensis* flies, which are resistant to DCV infection (supplementary fig. S2, Supplementary Material online). CrPV RNA accumulation was substantial in all species, in contrast with the marked differences mentioned above with DCV (Fig. 2). We note that CrPV viral RNA load is less predictive of survival than in the case of DCV, suggesting a stronger contribution of resilience/disease tolerance during

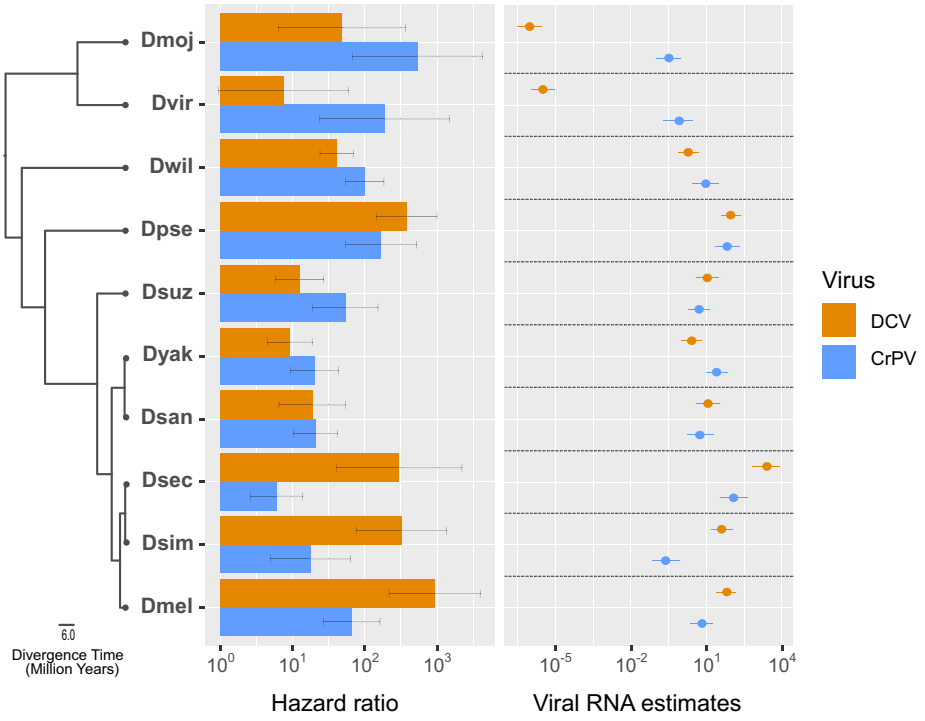

Fig. 2. Susceptibility of *Drosophila* species to infection is virus specific and related to phylogeny. Hazard ratio of the different fly species for DCV (top) or CrPV (bottom) infection relative to their Tris injected counterparts, based on a mixed effects Cox proportional hazards model. Confidence intervals (0.95) are indicated (left panel). Data are representative of supplementary figs S1 and S2, Supplementary Material online. Estimates of relative viral RNA level, based on Bayesian regression model with an underlying Student distribution, 3 d after infection of 3 or more independent experiments with 3 biological replicates. Credible intervals (0.95) are indicated (right panel). Dmel—*Drosophila (D.) melanogaster*; Dsim—*D. simulans*; Dsec—*D. sechellia*; Dsan - *D. santomea*; Dyak - *D. yakuba*; Dsuz - *D. suzukii*; Dpse - *D. pseudoobscura*; Dwil - *D. willistoni*; Dvir - *D. virilis*; Dmoj - *D. mojavensis*.

CrPV infection (Medzhitov et al. 2012) (supplementary fig. S2b, Supplementary Material online).

Overall, our data show that *Drosophila* species display different susceptibilities to *Dicistroviridae* infection. These are virus specific (e.g. *D. simulans* sensitive to DCV but resistant to CrPV), and partially consistent with phylogeny (e.g. *D. santomea*, *D. yakuba*, and *D. suzukii* showing similar phenotypes to both viruses).

2′3′-cGAMP Protects *Drosophila* Flies Against CrPV Infection Across Species

We next monitored expression of *STING* and *Nazo* 2- and 3-days post-DCV or -CrPV infection as a read-out for induction of STING signaling in response to viral infection. We previously reported that these 2 genes can be used as markers to monitor activation of the STING pathway in *D. melanogaster* (Goto et al. 2018; Cai et al. 2020) (note that *Nazo* is only present in the Sophophora clade). We observed induction of *STING* and/or *Nazo* by both viruses in 4 species: *D. santomea*, *D. yakuba*, *D. suzukii*, and *D. willistoni*. These genes were also induced after DCV infection in *D. melanogaster* and *D. sechellia*. By contrast, CrPV repressed *STING* expression in *D. virilis* and *D. mojavensis* (supplementary figs. S4 and S5, Supplementary Material online). We next injected the STING-agonist 2′3′-cGAMP into flies and monitored expression of *STING* and *Nazo* 24 h later. We observed induction of *STING* and/or *Nazo* in all species (supplementary fig. S6, Supplementary Material online). These data suggest that the STING pathway is functional in the *Drosophila* species tested.

To address the contribution of the STING pathway to the resistance to *Dicistroviridae* in flies besides *D. melanogaster*, we co-injected 2′3′-cGAMP with CrPV in flies from the different species. CrPV was chosen for these experiments as it replicates better in all the species (Fig. 2). 2′3′-cGAMP co-injection led to significant decrease in viral RNA 3 d postinfection in all the species (Fig. 3a). Accordingly, survival with CrPV infection was significantly improved by 2′3′-cGAMP in all the flies (Fig. 3b). Of note, this protection was variable among species, and was weaker in some of them (e.g. *D. sechellia* and *D. mojavensis*), as reported elsewhere in a study comparing the efficiency of different CDNs to protect flies against DCV infection (Cai et al. 2023). These results indicate that injection of 2′3′-cGAMP can induce antiviral immunity in a set of diverse *Drosophila* species and raise the question of the repertoire of antiviral genes induced in each species.

The Multispecies Transcriptome of the Response to 2′3′-cGAMP

Flies were injected with Tris buffer or 2′3′-cGAMP and their transcriptome was analyzed 24 h later by RNAseq. We observed differential gene expression in all species (Fig. 4A, supplementary table S1, Supplementary Material online),

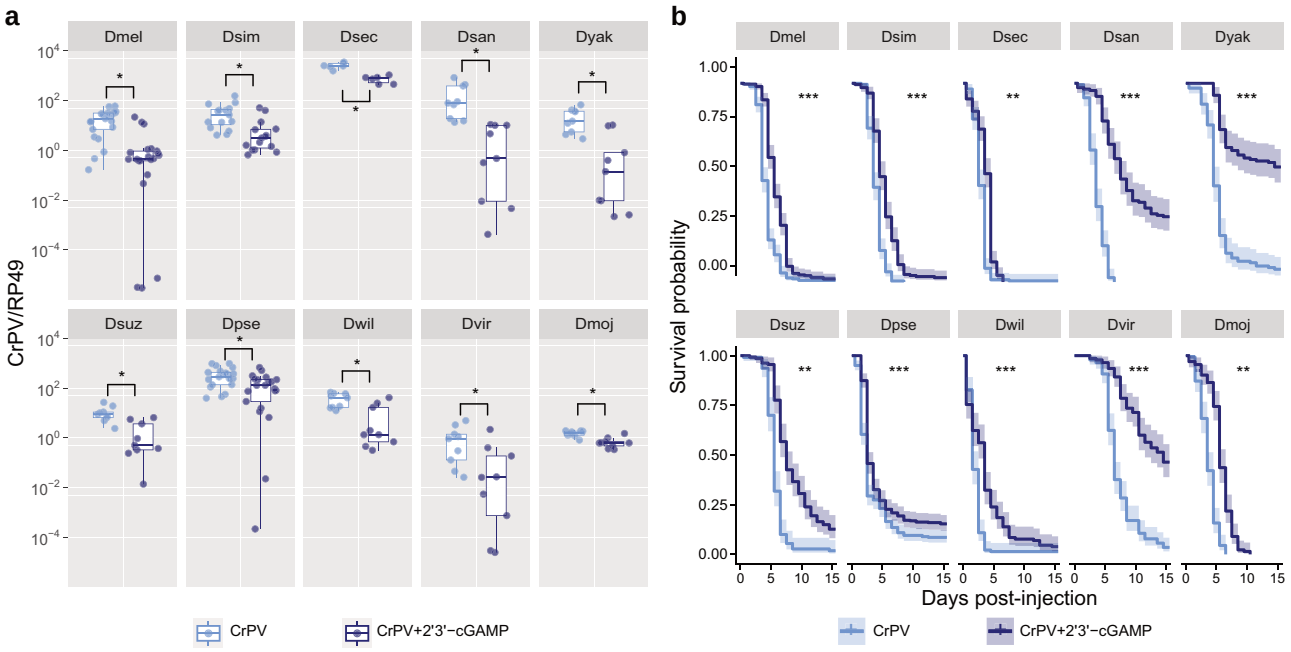

Fig. 3. 2′3′-cGAMP protects all *Drosophila* species tested against CrPV infection. a) Relative CrPV viral RNA levels 3 d after injection of CrPV alone or with 2′3′-cGAMP in 10 *Drosophila* species. Data are represented as boxplots of 3 or more independent experiments with 3 biological replicates. Individual dots represent samples of 5 male flies. Viral RNA levels between CrPV and 2′3-cGAMP + CrPV conditions were compared using a Bayesian regression model with an underlying Student distribution followed by pairwise comparisons. Species abbreviations are as in Fig. 2. * = credible interval for difference excludes 0; ns = credible interval includes 0 b) Kaplan–Meier survival curves of CrPV or CrPV with 2′3′-cGAMP injected flies. Curves were compared using a mixed effects Cox proportional hazards model *$P < 0.01$; **$P < 0.01$; ***$P < 0.001$.

which was validated by RT-qPCR on an independent set of samples for a subset of 5 genes (supplementary fig. S7, Supplementary Material online). In the reference species, *D. melanogaster*, we observed 72 differentially expressed genes (DEGs) (36 up- and 36 down-regulated genes). These numbers are reduced compared to our previous study (115 and 63 genes induced or repressed respectively) (Cai et al. 2020), which likely reflects the fact that the dose and volume injected were lower in this study (see Material and Methods) (supplementary fig. S8, Supplementary Material online). DEGs were also observed in all the other species, with the strongest inducible response observed in *D. willistoni* (79 up-regulated genes), *D. sechellia* (72 up-regulated genes), and *D. yakuba* (73 up-regulated genes). By contrast, only 21 up-regulated genes were observed in *D. simulans*. 2′3′-cGAMP also repressed gene expression in all species except *D. mojavensis*. Overall, the number of down-regulated genes was lower than the number of induced genes, with the notable exception of *D. willistoni* (more down-regulated genes), *D. simulans* (near-equal numbers), and *D. melanogaster* (equal numbers). These data pave the way for a comparative analysis of the STING-regulated genes in different *Drosophila* species.

The Core of 2′3′-cGAMP Induced Genes Includes Known Antiviral Effectors

To compare the sets of DEGs across the 10 species, orthologs, and paralogs were identified from the DrosOMA *Drosophila* Orthologous Matrix browser (Thiébaut et al. 2023). DrosOMA delineates orthology for 36 drosophilids from across the genus, providing Hierarchical Orthologous Groups (HOGs) comprising sets of genes descended from a single ancestral gene in a last common ancestor. Comparing the responses in the different species via orthology with HOGs containing DEGs in at least one species shows positive correlations with variable-strength that are largely significant. These correlations increase when requiring DEGs in at least 2 species and generally decline with growing divergence times between species (Fig. 4b and c). To focus on HOGs containing 2′3′-cGAMP-responsive genes, the HOGs were filtered to select those where more than half of the member genes from the 10 species showed significant differential expression (up- or down-regulated). This identified a total of 31 HOGs (Fig. 5), 17 of which have orthologs in all 10 species - 10 HOGs with a single ortholog in each species, 2 with paralogs in some species, and 5 with paralogs in all species. Strikingly, the only gene present and induced in all species is *pastrel* (*pst*), which was previously characterized as a restriction factor for *Dicistroviridae* (Magwire et al. 2012; Martins et al. 2014; Cao et al. 2017). This gene is weakly induced in *D. melanogaster* compared to the other species, illustrating the added value of this comparative approach. Other known immune genes are also induced in most species. We previously reported that *Argonaute* (*AGO*)*2*, encoding a key component of the siRNAi pathway, was up-regulated in *D. melanogaster* by 2′3′-cGAMP treatment (Cai et al. 2020). Similar results were obtained in this study,

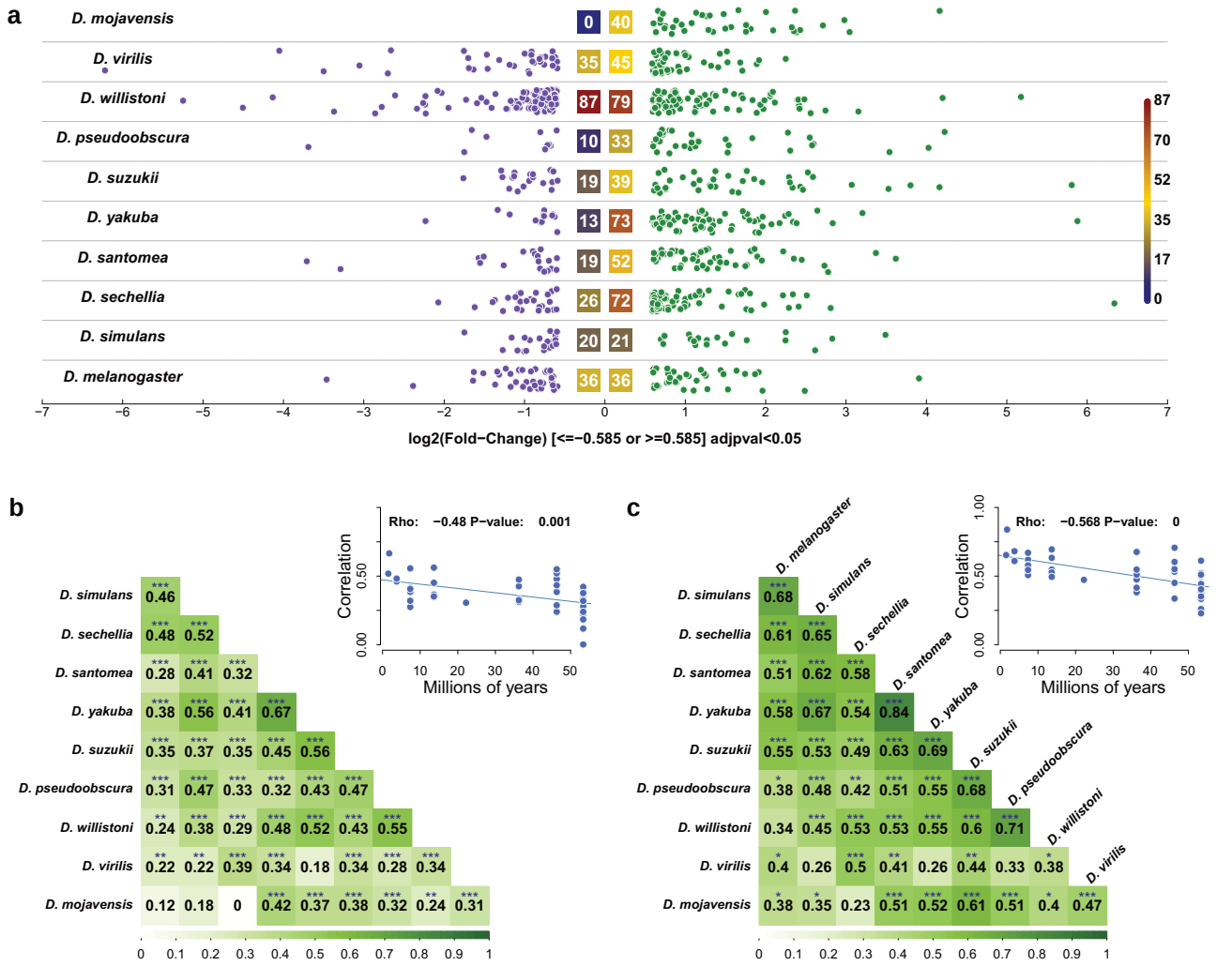

Fig. 4. Overview of the multispecies analysis of the transcriptional response to 2′3′-cGAMP. a) Dotplot of DEGs in each species as determined by multispecies RNAseq analysis 24 h postinjection of 2′3-cGAMP. Each dot represents a DEG scattered by log2 FC (≤−0.585 or ≥0.585 and adjusted *P*-value < 0.05). The overall number of dots is indicated with color-coded boxes based on the numbers of up-regulated DEGs (right) and down-regulated DEGs (left). Most species show more up-regulated genes than down-regulated genes, apart from *Drosophila melanogaster* (equal), *D. simulans* (near-equal), and *D. willistoni* (more down-regulated genes). Spearman correlations between species of gene expression changes based on b) 400 HOGs with DEGs in at least 1 species and c) 113 HOGs with DEGs in at least 2 species. Significance thresholds: **P* < 0.001; ***P* < 0.0001; ****P* < 0.00001. Inset plots in panels b and c contrast the pairwise correlation coefficients with the estimated divergence times between species, showing decreasing expression correlation with increasing evolutionary divergence.

demonstrating *AGO2* induction in 7 other species. Of note, we find that Dicer-2, which acts upstream of AGO2 in the siRNA pathway, and is not induced in *D. melanogaster*, is induced in 6 of the 10 *Drosophila* species tested. Signaling molecules were also present among the HOGs of interest, including *STING* itself, which is up-regulated in 6 species, *kenny* (*key*), which encodes the homolog of NF-Kappa-B essential modulator/IKKγ, the regulatory subunit of the IκB kinase (inhibitor of nuclear factor kappa-B kinase [IKK]) complex (Rutschmann et al. 2000) and the IκB-like molecule *Charon* (Ji et al. 2016; Morris et al. 2016) (both induced in 9/10 species). Notably, 1 HOG corresponds to the gene *CG7194*, which encodes the third cGAS-like-receptor present in *D. melanogaster*, GLR3 (Wu et al. 2014; Holleufer et al. 2021; Cai et al. 2023). This gene is not up-regulated in *D. melanogaster* but is induced in 5 of the 8 species where it is present. Remarkably, the gene has been duplicated in some species with 2 copies in *D. santomea*, *D. yakuba*, and *D. pseudoobscura* and 3 copies in *D. suzukii*, which are all induced except one of the paralogs in *D. yakuba*. Finally, the antiviral gene *Vago* (Deddouche et al. 2008) is induced by 2′3′-cGAMP in 7 of the 10 tested species.

Besides genes with known antiviral roles, some HOGs include uncharacterized *D. melanogaster* genes. Among these *CG14499* and *CG14500*, which are predicted to encode C-type-lectins, are DE in 6 species. Interestingly, these genes have been duplicated in a subset of species (*D. melanogaster*, *D. simulans*, *D. yakuba*, and *D. santomea*) and all but 1 paralog is up-regulated. Other candidates emerging from this comparative expression screen include *CG17224* (a predicted uridine phosphorylase induced in

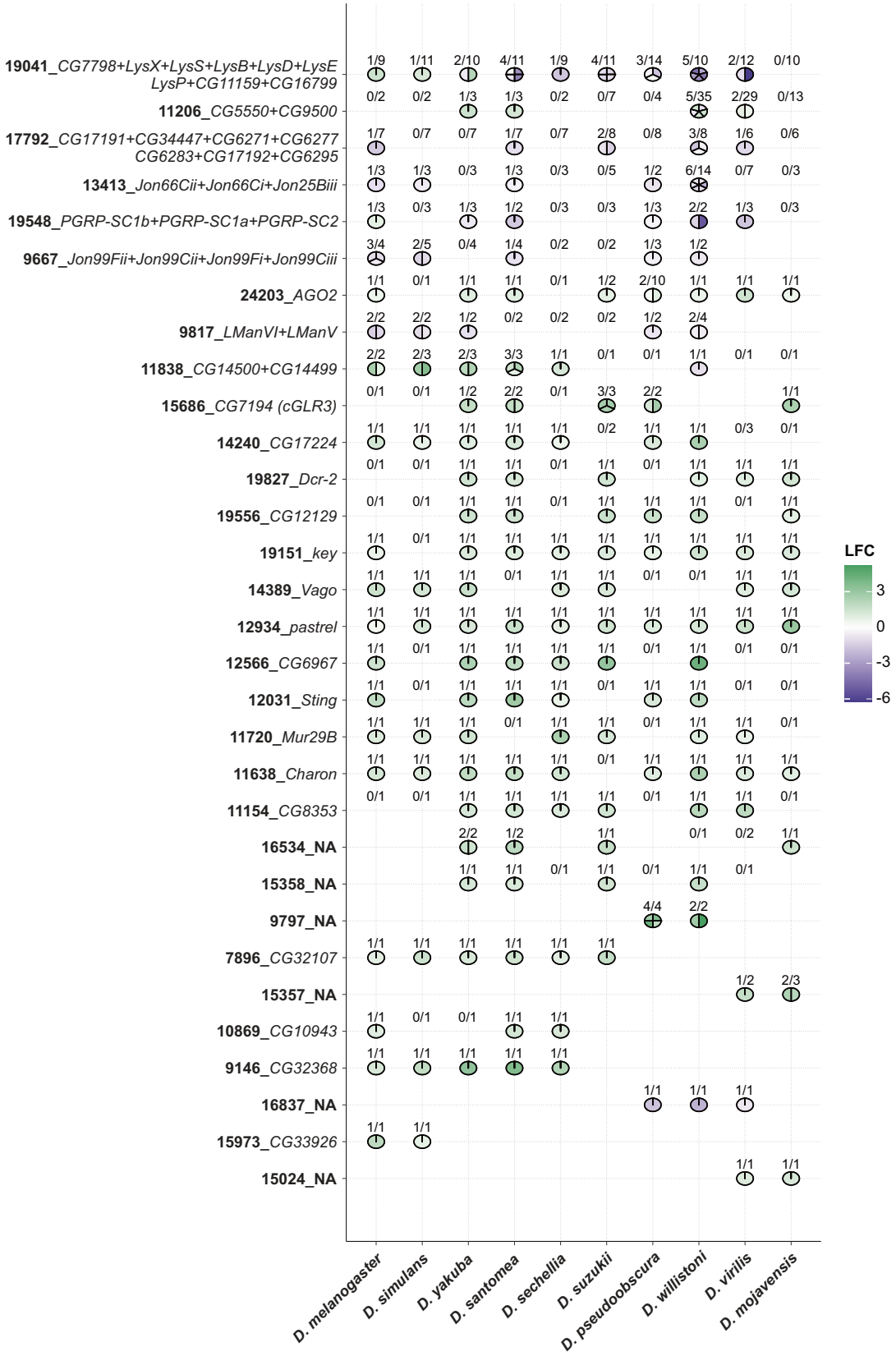

Fig. 5. Multispecies analysis reveals a conserved core of 2′3′-cGAMP regulated genes in Drosophilids. RNA-sequencing data of 10 *Drosophila* species injected with the STING agonist 2′3′-cGAMP or a mock injection. On the X axis are represented the species ordered by evolutionary distance to *D. melanogaster*. On the Y axis, the HOG number is indicated in bold, followed in italics by the name of the *D. melanogaster* gene, when it exists. For each species and HOG group a fraction indicates the number of DE paralogs over the total number of paralogs and a pie chart indicates the log fold-change (LFC) for each DE gene.

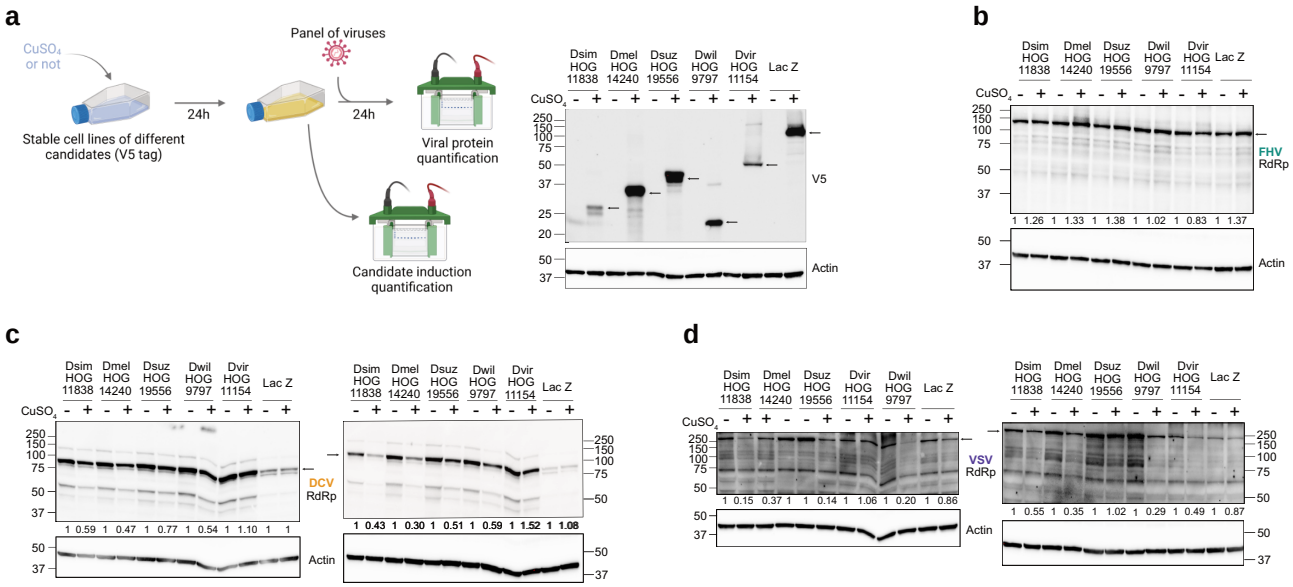

Fig. 6. Dsim HOG 11838, Dmel HOG 14240, and dwil HOG 9797 seem to protect against DCV and VSV in S2 cells. a) Schematic of the infection protocol. a to d) Stable cell populations expressing different RNAseq candidates tagged with V5 under a copper inducible promoter were tested for proteins of interest (POI) expression (a) and infected with FHV (b), DCV (c), and VSV (d). The cell lysates prepared 24 hr after copper induction (a) or 24 hr after infection (b to d) were analyzed by immunoblot using the indicated antibodies. The molecular weight of the ladder proteins is indicated in kiloDalton (kDa) and bands at expected size are indicated by an arrow. Relative levels of viral RNA-dependent RNA polymerase (RdRp) are indicated below the lane. Cell lines are annotated by species of origin of the expressed gene and HOG number of the candidate expressed by the cell line. For tested gene names see supplementary table S3, Supplementary Material online.

7/10 species), *CG12129* (predicted role in transcription and RNA binding, induced in 6/10 species), *CG6967* (a helicase related to the RNA induced silencing complex component (RISC) MOV10 (Arora et al. 2022; Liu et al. 2023), induced in 6/10 species) and *CG8353* (a predicted cytidine deaminase induced in 6/10 species). To test the antiviral activity of candidates, we constructed expression vectors for members of the HOGs 11838, 14240, 19556, and 11154, established stable cell lines and infected them with 3 viruses sensitive to the activation of the STING pathway, DCV, Vesicular Stomatitis Virus (VSV; *Rhabdoviridae*) and Flock House Virus (FHV; *Nodaviridae*) (Fig. 6a) (Cai et al. 2020). None of the candidates affected accumulation of the RNA-dependent RNA polymerase from FHV (Fig. 6b). Interestingly, ectopic expression of the representative of HOG14240 (predicted uridine phosphorylase) resulted in a 50% reduction of expression of the viral polymerase from DCV in 2 independent experiments (Fig. 6c). Expression of this gene also resulted in a more than 3-fold decrease in the expression of the polymerase from VSV in 2 independent experiments (Fig. 6d). Expression of a member of HOG11838 (predicted lectin type C) also resulted in reproducible decrease in the expression of the viral polymerases from DCV and VSV (Fig. 6c and d). Ectopic expression of the 2 other candidates (HOG11154 and 19556) gave less pronounced or reproducible effects.

DEGs from HOGs with 8 or more species also comprised down-regulated genes (e.g. the *Jon66C/25B* and *Jon99* families, encoding trypsin-like proteases, the L-mannosidases V and VI and the genes in HOG17792, predicted to encode phospholipases). More complex patterns of expression were also observed with a mixture of up- and down-regulated genes depending on the species (e.g. lysozymes in HOG19041). Overall, our analysis reveals that the core of 2′3′-cGAMP-induced genes includes known antiviral effectors, together with novel genes with putative antiviral functions.

Lineage-Specific HOGs Point to Potential Innovations in STING-Dependent Immunity

Several of the 2′3′-cGAMP-responsive HOGs encompass genes only present in clade-specific subsets, representing putative lineage-specific antiviral novelties. For example, HOG15357 and HOG15024 are restricted to species of the Drosophila subgenus, with genes up-regulated in both *D. virilis* and *D. mojavensis*. Conversely, genes from HOG7896 and HOG9146 are present and are all up-regulated in species belonging to the melanogaster group of the Sophophora subgenus (Fig. 5). HOG10869 is also restricted to Sophophora species, where the genes are up-regulated in 3 of the 5 tested species. Restricted to a subset of Sophophora including members of the obscura group, HOG9797 contains several paralogs, where all 4 *D. pseudoobscura* genes and both *D. willistoni* genes are up-regulated. HOG15357 is a putative MOV10 helicase and is restricted to the Drosophila subgenus, where 1/2 and 2/3 paralogs are up-regulated in *D. virilis* and *D. mojavensis*, respectively. Interestingly, the other putative MOV10 helicase (HOG12566) has a single gene in each of the 10

species (CG6967 in *D. melanogaster*), but the *D. virilis* and *D. mojavensis* orthologs are not up-regulated. This could suggest that the conserved single-copy ortholog has been "functionally replaced" by the lineage-specific group of MOV10 helicases that emerged in species of the Drosophila subgenus. To assess a putative antiviral function for these lineage-specific genes, we ectopically expressed 1 of the 2 paralogs of HOG9797 in *D. willistoni* in S2 cells and tested the impact on viral infection. Interestingly, we observed a reproducible reduction in the expression of DCV and VSV polymerases (Fig. 6c and d), which was modest in the case of DCV but more consistent for VSV. No inhibition was observed for the third virus, FHV (Fig. 6b). The identification of several potential innovations in STING-dependent immunity, one of which appears able to suppress expression of viral proteins in transfected cells, highlights the dynamic evolution of antiviral effectors and the importance of investigations across multiple species.

Discussion

Here, we have investigated the repertoire of 2′3′-cGAMP-regulated genes in a panel of 10 *Drosophila* species with different susceptibilities to viral infection, after verifying that co-injection of the CDN protected the flies against CrPV, an insect virus with a broad host range in laboratory conditions (Plus et al. 1978). Globally, we found similar results to 2 studies where a large number of Drosophilids species was assayed for susceptibility to DCV and CrPV (Longdon et al. 2015; Imrie et al. 2021), namely: a large diversity of the susceptibility profiles to these virus; a positive correlation between survival and viral titers to DCV; a lack of correlation of susceptibility with the distance to the original isolation host (Longdon et al. 2015); and, in some species (e.g. *D. simulans*), little relationship between the susceptibility to these closely related viruses (Imrie et al. 2021). However, the sampling of only 10 species limited the power to formally validate some of these correlations. While raising flies with different food specialization or preferences on the same medium potentially limited the diversity of diet-related immune responses, a recent study demonstrated that the composition of protein and carbohydrate in the diet does not affect the susceptibility of drosophila species to viral infections (Roberts and Longdon 2021).

Our data confirm that gene expression can be induced by injection of 2′3′-cGAMP in a broad range of *Drosophila* species. Based on genetic data in mammals, *D. melanogaster* and the choanoflagellate *Monosiga brevicollis*, this activation is likely mediated by STING, although this will need to be validated by further studies (Wu et al. 2013; Cai et al. 2020; Woznica et al. 2021). By analogy with *D. melanogaster*, in which Relish is required for both antiviral immunity and 2′3′-cGAMP-dependent gene expression (Cai et al. 2020), we posit that at least a subset of the induced genes encode factors that participate in the control of viral infections. Since this study was initiated in 2020, the characterization of cGAS-like receptors (cGLRs) in *Drosophila* has revealed that they can produce 3 additional CDNs in vitro and in vivo, namely 3′2′-cGAMP, 2′3′-c-diAMP, and 2′3′-c-diGMP (Holleufer et al. 2021; Slavik et al. 2021; Cai et al. 2023). All these CDNs can trigger antiviral protection in *D. melanogaster*, albeit with different efficiencies (2′3′-c-diGMP > 3′2′-cGAMP > 2′3′-c-diAMP > 2′3′-cGAMP), and differences between *Drosophila* species were noted (Cai et al. 2023). Therefore, further studies are needed to identify the best CDN to trigger the most effective antiviral response in each species. Nevertheless, this first report on the response to 2′3′-cGAMP, the canonical animal CDN, provides valuable information and comparative analysis of the DEGs from our panel of species uncovers details, and highlights trends to support 3 major observations.

First, the comparison of DEGs among species reveals a core set of induced genes, pointing to fundamental functions associated with antiviral protection in drosophilids. Remarkably, the only gene that was found induced in all species is *pst*. Had this gene not been previously identified through genome wide association study analysis and host adaptation studies as a major restriction factor for *Dicistroviridae* in *D. melanogaster* (Magwire et al. 2012; Martins et al. 2014; Cao et al. 2017), our approach would certainly have made it a primary candidate for further functional characterization. Besides *pst*, other core genes include *STING* itself, but also the antiviral gene *Vago* (Deddouche et al. 2008) and the gene *CG7194*, encoding cGLR3 in *D. melanogaster*. Phenotypic characterization of flies mutant for *CG7194* or ectopically expressing the gene so far failed to reveal a function for cGLR3 in antiviral immunity (Martin et al. 2018; Holleufer et al. 2021), but the upregulation of the gene by 2′3′-cGAMP in half of the species indicates that a closer look at this gene is warranted. Of note, we recently observed residual CDN production in virus-infected *cGLR1/2* double mutant flies, making cGLR3 a prime candidate for their production (Cai et al. 2023). Other genes in the core set have not been previously characterized and represent prime candidates for further characterization to identify novel immune factors, both regulatory components of the cGLR/STING pathway (e.g. *Charon*, *key*) and restriction factors (e.g. *CG12129*, *CG17224*, *CG6967*, *CG8353*). In this regard, the reproducible inhibition of expression of the viral polymerase of 2 of the 3 viruses tested observed with orthologs from *CG14499/CG14500* and *CG17224*, 2 of the 4 candidates tested, is promising.

Second, our analysis reveals that 2 of the 3 key components of the siRNA pathway, AGO2, and Dicer-2, are in the core set of 2′3′-cGAMP-induced genes. This suggests a connection between the STING-dependent induced response and antiviral RNAi that needs to be addressed to obtain the full picture of the integrative response to viral infection in *Drosophila*. This raises several questions including: do the siRNA and STING pathways operate in the same cells or do they protect distinct types of tissues, as suggested by recent reports revealing that the siRNA

pathway does not protect some tissues, e.g. digestive tract, against viruses (Carissimo et al. 2015; Mondotte et al. 2018; Olmo et al. 2018)? Are induced antiviral immunity and antiviral RNA silencing incompatible in the same cells, as reported in mammals (Girardi et al. 2015; Maillard et al. 2016; Veen et al. 2018)? Is there a hierarchy between antiviral RNAi and STING-dependent immunity, with the STING pathway kicking in only when RNAi fails to clear the infection?

Finally, our study reveals genes that are responsive to 2′3′-cGAMP only in some species or some groups. This illustrates the potential of comparative approaches to exploit the extensive biodiversity generated during evolution. A similar study investigated the response of fibroblasts from 10 different species of vertebrates to treatment with type I IFN. Besides a core set of 62 ISGs up-regulated in all species, this report also noted a number of ISGs induced in specific clades or species, revealing genes that had not been previously associated with the response to viral infections (Shaw et al. 2017). Interestingly, some of the lineage-specific genes we identified have been duplicated, yielding 2 to 4 paralogs per species (e.g. HOG16534, HOG9797, and HOG15357). This may be advantageous for the flies as it offers the possibility to target a virus or viral family by immunity factors with overlapping restriction features, decreasing the chances of escape by a single mutation event in the virus (Tenthorey et al. 2022). It is particularly encouraging that we observed a reproducible antiviral activity on both DCV and VSV in cells expressing 1 paralog from the HOG9797 group. Such uncharacterized genes identified in nonmodel species may play fundamental roles in the control of some families of viruses (McDougal et al. 2022). In a context where the threat of new viral pandemics is ever present (Dobson et al. 2020; Gibb et al. 2020), with the corresponding need for new antiviral strategies, investigating the function of genes from lineage-specific HOGs like HOG9797 or HOG9146, albeit challenging, may reveal unique antiviral strategies that can be harnessed for therapeutic purposes (Imler et al. 2024).

Materials and Methods

Drosophila Strains

All fly stocks used (*Drosophila melanogaster* w^{1118} line, *D. simulans*, *D. sechellia*, *D. santomea*, *D. yakuba*, *D. suzukii*, *D. pseudoobscura*, *D. willistoni*, *D. virilis*, and *D. mojavensis*) were raised on standard cornmeal agar medium at 25 °C and were free of *Wolbachia*. The different species of *Drosophila* were kindly provided by Prof. Dr. Nicolas Gompel (*D. simulans*, *D. sechellia*, *D. santomea*, *D. yakuba*, *D. pseudoobscura*, and *D. willistoni*); Dr. Eric Marois (*D. suzukii*) or ordered at the National Drosophila Species Stock Center (*D. virilis*, 15010-1051.48 and *D. mojavensis*, 15081-1352.47). For *D. melanogaster*, we used a laboratory-adapted mutant strain (*white* gene, affecting eye pigmentation) because (i) this line was used as the genetic background to characterize the phenotype of STING mutant flies, and (ii) resistance against DCV and CrPV is influenced by the *pastrel* genotype, which led us to use a fly strain with a susceptible genetic background for this restriction factor (Magwire et al. 2012; Martins et al. 2014; Cao et al. 2017). Host phylogeny reconstruction was based on Thiébaut et al. (2023). Male adult flies, collected 3- to 5-days post eclosion, were used in all experiments. All flies were anesthetized with CO_2 diffusion pads except *D. willistoni* for which cold pads were used.

Sensitivity of 10 Drosophila Species to Drosophila C and Cricket Paralysis Virus and Signaling Analysis

Three- to five-day-old adult male flies were infected with 4.6 nL of viral suspension in 10 mM Tris–HCl, pH 7.5 (Tris–HCl) of DCV (Sabatier et al. 2003) (5 plaque forming units [pfu]) or CrPV (5pfu) or just Tris–HCl by intrathoracic injection (Nanoject II apparatus, Drummond Scientific). For survival experiments, flies were monitored daily over 22 d; flies were flipped into new vials every 3 d to avoid bacterial proliferation. For RNA isolation, flies were collected 2- or 3-d postinfection in pools of 5 individuals and homogenized by Precellys Evolution (Bertin technologies with the following program: 2 cycles of 15 s at 5800 rpm with a pause of 30 s in-between) in TRIzol (Ambion) for RNA extraction with isoamyl chloroform (Sigma-Aldrich). RNA was used for quantitative PCR with reverse transcription (RT–qPCR) using the iScript gDNA Clear cDNA Synthesis (Bio-Rad) or the gDNAOut OneScript (Ozyme) kit and the iTaq Universal commercial product Green Supermix (Bio-Rad), according to the manufacturer's instructions. For each sample, 2 technical replicates were performed for each amplicon (viral and *Rp49*/*RPL32*). RP49 and gene of interest (GOI) primers specific to groups of species were used (supplementary table S2, Supplementary Material online). Primer efficiency was determined by performing a serial dilution of a combination of infected and uninfected samples from multiple experiments conducted for each species.

Antiviral Effect of 2′3′-cGAMP in 10 *Drosophila* Species

2′3′-cGAMP (InvivoGen) was diluted to 0.9 µg/µL in 10 mM Tris–HCl pH 7.5. 3 to 5 d old adult male flies were injected by intrathoracic injection (Nanoject II apparatus, Drummond Scientific) with 13.8 nL of a mix of 4.6 nL of CrPV (5 PFU) and 9.2nL of either 2′3′-cGAMP (0.9 µg/µL) or Tris–HCl. The species *D. simulans* and *D. sechellia*, which were found to be less susceptible to CrPV infection, were injected with 50 PFU instead of 5 PFU to remain in the dynamic range of the protection assay. As controls, flies were injected with Tris–HCl or a mix of 4.6nL of Tris–HCl and 9.2nL of 2′3′-cGAMP (0.9 µg/µL). For survival experiments flies were monitored daily over 15 d; flies were flipped into new vials every 3 d to avoid bacterial proliferation. For RNA isolation, flies have collected 3 d postinjection in pools of 5 individuals and homogenized for RNA extraction and quantitative PCR with reverse transcription (RT–qPCR) analysis, as described above.

2′3′-cGAMP Injection and Signaling Analysis in 10 *Drosophila* Species

2′3′-cGAMP was diluted to 0.9 µg/µL in 10 mM Tris–HCl pH 7.5. 3 to 5 d old adult male flies were injected by intrathoracic injection (Nanoject II) with 13.8 nL of Tris–HCl or a mix of 4.6 nL of Tris–HCl and 9.2 nL of 2′3′-cGAMP (0.9 µg/µL). For RNA isolation, flies were collected 3 days post injection in pools of 5 individuals and homogenized for RNA extraction and RT–qPCR analysis, as described above. For the validation of the RNAseq data, 69 nL of 2′3′-cGAMP (Biolog C161) dissolved in 10 mM Tris–HCl pH 7.5 and diluted at the indicated concentration were injected in 3 to 5-d old adult flies. Flies were collected 1 d later in pools of 6 individuals (6 males) and homogenized for RNA extraction and RT–qPCR analysis, as described.

RNA-Sequencing of *Drosophila* Flies Injected with 2'3'-cGAMP

Three to five days old adult male flies from each species were injected by intrathoracic injection (Nanoject II apparatus) with 13.8 nL of Tris–HCl or a mix of 4.6 nL of Tris–HCl and 9.2 nL of 2′3′-cGAMP (0.9 µg/µL) in 3 independent experiments. Injected flies were collected in pools of 5 individuals 24 h post injection. Total RNA was isolated from injected flies using TRIzol Reagent (Ambion), according to the manufacturer's protocol. RNA quality was assessed on an Agilent 2100 Bioanalyzer (Agilent Technologies, Palo Alto, CA, USA). After total RNA was extracted, eukaryotic mRNA was enriched by Oligo(dT) beads. Then, the enriched mRNA was fragmented into short fragments using fragmentation buffer and reverse transcribed into cDNA by using NEBNext Ultra RNA Library Prep Kit for Illumina (NEB #7530, New England Biolabs, Ipswich, MA, USA). The purified double-stranded cDNA fragments were end repaired, A base added, and ligated to Illumina sequencing adapters. The ligation reaction was purified with the AMPure XP Beads (1.0X). Ligated fragments were subjected to size selection by agarose gel electrophoresis and polymerase chain reaction (PCR) amplified. The resulting cDNA libraries were sequenced in a Illumina NovaSeq6000 by Gene Denovo Biotechnology Co. (Guangzhou, China).

Gateway Constructs

To establish plasmids expressing genes of interest (GOI), mRNA was isolated as described above from the different species injected with a mix of 4.6 nL of Tris–HCl and 9.2 nL of 2′3′-cGAMP (0.9 µg/µL). 1 µg of RNA was retrotranscribed into cDNA using the Superscript IV RT kit (Invitrogen) and Oligo d(T)20 primers following the manufacturer's instructions. Gene(s) of interest (GOIs) were amplified from cDNA and PCR products were analysed on 1% agarose gels. The expected bands were cut from the gel and purified with the QIAquick Gel extraction kit (Qiagen). Purified PCR products were subcloned into pJET (Thermoscientific) cloning vectors. GOIs were then amplified from pJET constructs with attB sites for Gateway cloning. The BP reaction was done using the gel purified PCR product, Kanamycin-resistant pDONOR221-vectors, and the Gateway BP Clonase II (Invitrogen) to establish entry plasmids (pENTR). For the attL/attR site specific recombination (LR) cloning, pENTRs were combined with a Ampicilin-resistant destination plasmids (pDEST) to generate the final Expression plasmids (pEXP) using the LR Clonase II (Invitrogen). The pDEST was a modified pMTV5-HisA (ThermoFisher) to which a Gateway cassette was added in the multiple cloning sites region between the promoter and the tag. All final plasmids and intermediates were amplified by mini or midiprep using QIAprep Spin Miniprep kit or the QIAfilter Plasmid Midi kit (Qiagen) according to manufacturer's instructions. GOI sequences were validated by Sanger sequencing (Eurofins). Proper expression of proteins was tested by western blot as described above. Candidates tested were selected based on their optimal combination of high induction and extensive RNAseq coverage. Primers used for cloning can be found in supplementary table S3, Supplementary Material online.

Stable Cell Lines and Viral Infections

Stable cell lines expressing the GOI were derived from S2 cells transfected with plasmids coding for the C-terminally V5-tagged candidate protein under the control of the metallothionein promoter and the puromycin resistance gene. Protein expression was induced using 0.5 mM $CuSO_4$ containing culture medium for 24 h at 25 °C. GOI expression was tested by Western blot. For viral infection, cells were resuspended in 200 µL of viral suspension diluted in non-supplemented Schneider (without fetal bovine serum). DCV was used at a multiplicity of infection (MOI) of 0.01, FHV at an MOI of 0.1, and VSV at an MOI of 1. Virus was adsorbed for 1 h at 25 °C in Eppendorf tubes inverted every 10 min to avoid cell sedimentation. After adsorption, cells were cultured in complete Schneider media for the indicated times.

Protein Extraction and Western Blot Analysis

Cells were homogenized in Lysis Buffer containing 4-(2-hydroxyethyl)-1-piperazineethanesulfonicacid KOH pH 7.5 buffer (30 mM), NaCl (150 mM), Mg(OAc)2 (2 mM), 1% IGEPAL (Euromedex), mixed with 2 × protease inhibitor (PI) (Roche). After 30 min incubation on ice, cell lysate was centrifuged for 15 min at 10,000 × *g* at 4 °C and the supernatant was collected in new Eppendorf tubes. Proteins were quantified spectrophotometrically by Bradford Protein assay (Biorad) or Bicinchoninic acid assay (Milipore). Thirty micrograms of sample were mixed with MilliQ water, Laemmli sample buffer (Bio-Rad) 1X, and 10 mM dithiothreitol in 30 µL of final volume. Mix was incubated for 5 min at 95 °C and applied to 4% to 15% Mini-PROTEAN TGX Stain-Free gels or 8% to 16% Criterion TGX Stain-Free gels (BioRad). Migration of samples was performed in 1X Tris-Glycine-sodium dodecyl

sulfate buffer (Euromedex) at 80 V and gels were stain-free activated using the ChemiDoc Imaging System (Bio-Rad). Proteins were transferred to nitrocellulose membranes for 30 min at 25 V and 1.0A with a Trans-Blot Turbo transfer system (Bio-Rad). Transfer of proteins to the membranes was verified by incubating with Stain-free method. Primary monoclonal mouse antibodies against (α) V5-horse radish peroxidase (HRP) (Invitrogen) or actin (Euromedex) were diluted 1:10,000 or 1:1,000, respectively, the mouse α-actin (Gene Tex) and guineapig raised antibodies α-DCV and α-VSV RNA-dependent Rdrp (custom made by ProteoGenix) were diluted 1:2,000. Guineapig antibodies α-FHV Rdrp (custom made by ProteoGenix) and secondary antibodies α-mouse IgG- or guineapig IgG-HRP (Amersham) were diluted 1:10,000. Chemiluminescence was detected using a Chemidoc Imaging System (Bio-Rad). Western blots were quantified using ImageLab 6.1 and normalized by the actin bands.

RNA-Sequencing Analysis

The RNAseq data were analyzed using the workflow https://gitlab.com/aathbt/rnaseq-analysis-workflow/at commit e721a286. Unless specified otherwise, default parameters were used. Briefly, reads were quality-checked with FastQC v.0.11.9 (Andrews 2010) before and after trimming. Sequencing error-rate was estimated using "*atropos error*" from Atropos v1.1.28 (Didion et al. 2017). Adapters were detected using "*atropos detect*" from Atropos with the "–no-cache-contaminants' parameter. Adapters and low-quality reads were trimmed using "*atropos trim*" from Atropos. Previously detected adapters were used as "-a/-A" parameters, as well as "A{20}". Previously computed error-rate was used as "-e" parameter. Other nondefault parameters were "-n 2 -q 20,20 –minimum-length 25 –trim-n –max-n 10 –no-cache-adapters'. The assembly indexes were built using "*hisat build*" from HISAT2 v.2.1.0 (Kim et al. 2015). The trimmed reads were aligned using HISAT2 against their respective assemblies with the parameters "–max-intronlen 120,000 –dta -k 10 –max-seeds 10 –no-mixed –no-discordant". Reads aligning at only 1 location in the assembly were selected using samtools v1.10 (Danecek et al. 2021). Read counts for each gene were produced using featureCounts v2.0.1 (Liao et al. 2014) with the parameters "-O –fraction -p -P -B -C" and the annotations described in the supplementary table S4, Supplementary Material online. Beforehand, each annotation file was quality-checked and fixed using AGAT v0.5.1 (Dainat et al. 2020). Differential expression analyses were carried out under R v4.0.3 (R Core Team 2023) with the DESeq2 package v1.30.0 (Love et al. 2014). A "local" fit was used for the dispersion and a batch effect caused by replicates was included in the design formula. Genes with an expression |fold-change (FC)| ≥ 1.5 (equivalent to |log2FC| ≥ 0.585) and a Benjamini–Hochberg corrected *P*-value < 0.05 were considered DE. Expression response comparisons between pairs of species were performed using 400 HOGs with DEGs in at least 1 species and 113 HOGs with DEGs in at least 2 species. For HOGs containing multicopy orthologs, among pairs of orthologs the pair with the smallest difference in log2 FC was selected: if both species contained DEGs only considering DEG–DEG pairs; if only one of the species contained DEGs only considering DEG-ortholog pairs; and if neither species contained DEGs considering all ortholog pairs. Spearman correlations were performed using the Base R function cor.test(). RNAseq reads from each species was analyzed for the presence of viruses using the software Kraken2, which did not identify viral sequences.

Survival Analysis

Survival data were analyzed separately for each virus with a mixed-effects Cox proportional hazards model using coxme version 2.2-18.1 (Therneau 2022). The model incorporated species, treatment, and their interaction as fixed effects; to control for between-experiment and vial variation, experimental batch and individual vials were included as additional fixed and random effects. The final models had the form:

$$\text{coxme}(\text{Surv}(\text{time}, \text{status}) \sim \text{species} * \text{treatment} + \text{experiment} + (1|\text{vial}))$$

In the event that there was no instance of death for a given species/treatment/experimental batch combination, an artificial death was introduced on one fly per experiment at the end of the follow-up time (20 d) to allow convergence of the model and estimation of the hazard ratio. Hazards ratios between infected and noninfected conditions were then estimated for each species from the global model using emmeans (1.9.0 (Lenth 2023)) (supplementary table S5 and S6, Supplementary Material online). To obtain homogeneous groups, standardized effect-size measures were then estimated from the pairwise comparisons contrasts (indicated on supplementary figs. S1, S2 and table S5, Supplementary Material online); homogeneous groupings were determined using multcompView (version 0.1-9(Graves et al. 2023)). *P*-values lower than 0.05 were considered statistically significant and multiple comparison *P*-values were corrected using the false discovery rate method. Data were plotted and analyzed using R (4.3.2 (R Core Team 2023) and R studio (2023.12.0 (Posit team 2023)).

qPCR Analysis

Viral and gene mRNA levels were plotted and analyzed using R (4.3.2 (R Core Team 2023)) and R studio (2023.12.0 (Posit team 2023)). Primer efficiency corrected coefficient was calculated using the following formula using the slope of the serial dilutions (see above):

$$coeff = 10^{\left(\frac{-1}{slope}\right)}$$

Relative gene expression (ΔCq) was calculated with the following formula:

$$\Delta Cq = \frac{(coeff_{RP49})^{\overline{Cq}_{RP49}}}{(coeff_{gene})^{\overline{Cq}_{gene}}}$$

$\overline{Cq}$ = mean Cq of the technical duplicate

Gene fold-changes ($\Delta\Delta Cq$) were calculated with the following formula:

$$\Delta\Delta Cq = \frac{\Delta Cq_{(treated)}}{\overline{\Delta Cq}_{(ctrl)})}$$

$\overline{\Delta Cq}_{(ctrl)}$ = mean ΔCq of the controls biological replicates

ΔCqs were used for pairwise or multiple comparisons. Density distribution of the log10(ΔCq) residuals was analysed using ggplot2 (version 3.4.4 (Wickham 2016)). Statistical analysis was performed using a Bayesian model with an underlying student distribution with flat priors using brms (version 2.20.4 (Bürkner 2017; Bürkner 2018; Bürkner 2021)). The model incorporated species, treatment, days postinfections (dpi), and their interactions as fixed effects. Additionally, experiments were included as random effects to account for potential variability across experimental setups. The final model had the form:

$$\begin{aligned} \text{brm}(\log10(\text{deltaCq}) \sim\ & \text{species} * \text{dpi} * \text{treatment} \\ & + (1|\text{experiment}), \text{student}, \text{iter} \\ & = 100000) \end{aligned}$$

for the gene induction assays.

Credible intervals from the model were compared by pairwise comparison for each species and dpi between treatments using emmeans (1.9.0 (Lenth 2023)) (supplementary tables S7 to S13, Supplementary Material online). In case of multiple comparisons, standardized effect-size measures were then estimated from the pairwise comparisons contrast using emmeans (1.9.0 (Lenth 2023)) to compare viral titer or the effect of the treatment (virus or 2′3′-cGAMP injection) in gene expression (supplementary tables S7 and S8, Supplementary Material online). Compact letter displays were determined using multcompView (version 0.1-9 (Graves et al. 2023)).

To test the induction of RNAseq candidates upon 2′3′-cGAMP injection mRNA levels between and Tris conditions compared using Mann–Whitney tests. Credibility intervals excluding zeros were considered statistically significant, *P*-values lower than 0.05 were considered statistically significant and multiple comparison *P*-values were corrected using the false discovery rate method.

Correlation Analysis

Correlation between hazard ratio and back-traced viral RNA estimates using Spearman rank order correlation (cor.test in base R) was plotted and calculated using R (4.3.2 (R Core Team 2023)) and R studio (2023.12.0 (Posit team 2023)) (supplementary tables S5, S7 and S8, Supplementary Material online). To correlate the phylogenetic distance to *D. melanogaster* and survival or viral loads, the cophenetic distance between the different species of *D.melanogaster* was calculated from the species phylogeny using cophenetic.phylo in the "ape" package (version 5.7-1). The differences between log(hazard ratios) or log(Relative viral load) were then correlated with the distances using a Spearman rank order correlation (cor.test in base R).

Software and Packages Outside of RNAseq Analysis

Data preprocessing and statistical analysis were conducted using R (4.3.2 (R Core Team 2023)), R studio (2023.12.0 (Posit team 2023)) and the following packages: ape (5.7-1 (Paradis and Schliep 2019)), brms (version 2.20.4 (Bürkner 2017; Bürkner 2018; Bürkner 2021)), coda (version 0.19-4 (Plummer et al. 2006)), coxme (version 2.2-18.1 (Therneau 2022), data.table (1.14.10 (Dowel and Srinivasan 2023)), dplyr (version 2.4.0 (Wickham et al. 2023)), emmeans (1.9.0 (Lenth 2023)), geiger (2.0.11 (Alfaro et al. 2009; Pennell et al. 2014)), ggplot2 (version 3.4.4 (Wickham 2016)), gginnards (version 0.1.2) (Aphalo 2023), ggpubr (0.6.0 (Kassambara 2023a)), gplots (version 3.1.3), insight (version 0.19.7 (Lüdecke et al. 2019)), kableExtra (1.3.4 (Zhu 2021)), multcomp (1.4-25 (Hothorn et al. 2008)), multcompView (version 0.1-9 (Graves et al. 2023)), nlme (3.1-164 (Pinheiro et al. 2023)), phytools (2.1-1 (Revell 2012)), purr (1.0.2 (Wickham and Henry 2023)), readxl (1.4.3 (Wickham and Bryan 2023)), rstatix (0.7.2 (Kassambara 2023b)), scales (1.3.0 (Wickham and Seidel 2022)), stringr (1.5.0 (Wickham 2022)), survival (3.5-7 (Therneau 2023)), survminer (0.4.9 (Kassambara et al. 2021)), tidyverse (2.0.0 (Wickham et al. 2019)), tinytex (0.49 (Xie 2023)), and writexl (1.4.2 (Ooms and McNamara 2023)).

Supplementary Material

Supplementary material is available at *Molecular Biology and Evolution* online.

Acknowledgments

We thank Joao Marques for critical reading of the manuscript and useful advice, members of our laboratories in Strasbourg and Guangzhou and Ben Longdon for useful discussions and Florence Schlotter for expert technical assistance. We thank N. Gompel E. Marois for sharing the strains of the different drosophilids.

Funding

J.L.I. acknowledges financial support from Centre National de la Recherche Scientifique (France) and grants from Agence Nationale de la Recherche (ANR-10-IDEX-0002, ANR-11-EQPX-0022, ANR-17-EURE-0023, ANR-20-SFRI0012,

and ANR-22-CE15-0019). H.C. was supported by the National Natural Science Foundation of China (32000662, 32370767), Science Fund for Distinguished Young Scholars of Guangdong Province (2023B1515020098), Guangdong Provincial Young Scholars academic exchange program (2022A0505030018), Youth Talent Support Programme of Guangdong Provincial Association for Science and Technology (SKXRC202229), Guangzhou Municipal Science and Technology Project (202102020090). J.L.I. and H.C. acknowledge support by the Chinese National Overseas Expertise Introduction Center for Discipline Innovation (Project'111' (D18010)) and the National Key Research and Development Program of China (2023YFE010770). Work in the team of RMW was supported by the Swiss National Science Foundation grants 186397 and 202669.

Data Availability

RNAseq data from the different drosophila species injected with Tris or 2′3′-cGAMP are available at the European Nucleotide Archive, under the accession number PRJEB72191.

Data files and R scripts used in this study for qPCR and survival analysis are available at: https://git.unistra.fr/lhedelin/comparative-cgamp/.

References

Ablasser A, Chen ZJ. cGAS in action: expanding roles in immunity and inflammation. *Science*. 2019:**363**(6431):eaat8657. https://doi.org/10.1126/science.aat8657.

Adiliaghdam F, Basavappa M, Saunders TL, Harjanto D, Prior JT, Cronkite DA, Papavasiliou N, Jeffrey KL. A requirement for argonaute 4 in mammalian antiviral defense. *Cell Rep*. 2020:**30**(6):1690–1701.e4. https://doi.org/10.1016/j.celrep.2020.01.021.

Aguiar ERGR, Olmo RP, Marques JT. Virus-derived small RNAs: molecular footprints of host-pathogen interactions. *Wiley Interdiscip Rev RNA*. 2016:**7**(6):824–837. https://doi.org/10.1002/wrna.1361.

Alfaro ME, Santini F, Brock C, Alamillo H, Dornburg A, Rabosky DL, Carnevale G, Harmon LJ. Nine exceptional radiations plus high turnover explain species diversity in jawed vertebrates. *Proc Natl Acad Sci U S A*. 2009:**106**(32):13410–13414. https://doi.org/10.1073/pnas.0811087106.

Andrews S. 2010. Babraham Bioinformatics—FastQC A Quality Control tool for High Throughput Sequence Data. https://www.bioinformatics.babraham.ac.uk/projects/fastqc/.

Aphalo P. 2023. gginnards: Explore the Innards of "ggplot2" Objects. R package version 0.1.2. https://CRAN.R-project.org/package=gginnards.

Arora R, Bodak M, Penouty L, Hackman C, Ciaudo C. Sequestration of LINE-1 in cytosolic aggregates by MOV10 restricts retrotransposition. *EMBO Rep*. 2022:**23**(9):e54458. https://doi.org/10.15252/embr.202154458.

Bronkhorst AW, van Rij RP. The long and short of antiviral defense: small RNA-based immunity in insects. *Curr Opin Virol*. 2014:**7**:19–28. https://doi.org/10.1016/j.coviro.2014.03.010.

Bürkner P-C. Brms: an R package for Bayesian multilevel models using stan. *J Stat Softw*. 2017:**80**(1):1–28. https://doi.org/10.18637/jss.v080.i01.

Bürkner P-C. Advanced Bayesian multilevel modeling with the R package brms. *R Journal*. 2018:**10**(1):395–411. https://doi.org/10.32614/RJ-2018-017.

Bürkner P-C. Bayesian item response modeling in R with brms and stan. *J Stat Softw*. 2021:**100**(5):1–54. https://doi.org/10.18637/jss.v100.i05.

Cai H, Holleufer A, Simonsen B, Schneider J, Lemoine A, Gad HH, Huang J, Huang J, Chen D, Peng T, *et al.* 2′3′-cGAMP triggers a STING- and NF-κB-dependent broad antiviral response in Drosophila. *Sci Signal*. 2020:**13**(660):eabc4537. https://doi.org/10.1126/scisignal.abc4537.

Cai H, Li L, Slavik KM, Huang J, Yin T, Ai X, Hédelin L, Haas G, Xiang Z, Yang Y, *et al.* The virus-induced cyclic dinucleotide 2′3′-c-di-GMP mediates STING-dependent antiviral immunity in Drosophila. *Immunity*. 2023:**56**:1991–2005.e9. https://doi.org/10.1016/j.immuni.2023.08.006.

Cao C, Cogni R, Barbier V, Jiggins FM. Complex coding and regulatory polymorphisms in a restriction factor determine the susceptibility of Drosophila to viral infection. *Genetics*. 2017:**206**(4):2159–2173. https://doi.org/10.1534/genetics.117.201970.

Carissimo G, Pondeville E, McFarlane M, Dietrich I, Mitri C, Bischoff E, Antoniewski C, Bourgouin C, Failloux A-B, Kohl A, *et al.* Antiviral immunity of anopheles gambiae is highly compartmentalized, with distinct roles for RNA interference and gut microbiota. *Proc Natl Acad Sci U S A*. 2015:**112**(2):E176–E185. https://doi.org/10.1073/pnas.1412984112.

Daffis S, Szretter KJ, Schriewer J, Li J, Youn S, Errett J, Lin T-Y, Schneller S, Zust R, Dong H, *et al.* 2′-O methylation of the viral mRNA cap evades host restriction by IFIT family members. *Nature*. 2010:**468**(7322):452–456. https://doi.org/10.1038/nature09489.

Dainat J, Hereñú D, Pucholt P. 2020. NBISweden/AGAT: AGAT-v0.5.1. [Computer software]. Zenodo. https://zenodo.org/record/4205393

Dalskov L, Gad HH, Hartmann R. Viral recognition and the antiviral interferon response. *EMBO J*. 2023:**42**(14):e112907. https://doi.org/10.15252/embj.2022112907.

Danecek P, Bonfield JK, Liddle J, Marshall J, Ohan V, Pollard MO, Whitwham A, Keane T, McCarthy SA, Davies RM, *et al.* Twelve years of SAMtools and BCFtools. *Gigascience*. 2021:**10**(2):giab008. https://doi.org/10.1093/gigascience/giab008.

Daugherty MD, Malik HS. Rules of engagement: molecular insights from host-virus arms races. *Annu Rev Genet*. 2012:**46**(1):677–700. https://doi.org/10.1146/annurev-genet-110711-155522.

Deddouche S, Matt N, Budd A, Mueller S, Kemp C, Galiana-Arnoux D, Dostert C, Antoniewski C, Hoffmann JA, Imler J-L. The DExD/H-box helicase dicer-2 mediates the induction of antiviral activity in Drosophila. *Nat Immunol*. 2008:**9**(12):1425–1432. https://doi.org/10.1038/ni.1664.

Didion JP, Martin M, Collins FS. Atropos: specific, sensitive, and speedy trimming of sequencing reads. *PeerJ*. 2017:**5**:e3720. https://doi.org/10.7717/peerj.3720.

Dobson AP, Pimm SL, Hannah L, Kaufman L, Ahumada JA, Ando AW, Bernstein A, Busch J, Daszak P, Engelmann J, *et al.* Ecology and economics for pandemic prevention. *Science*. 2020:**369**(6502):379–381. https://doi.org/10.1126/science.abc3189.

Donelick HM, Talide L, Bellet M, Aruscavage PJ, Lauret E, Aguiar ERGR, Marques JT, Meignin C, Bass BL. In vitro studies provide insight into effects of dicer-2 helicase mutations in Drosophila melanogaster. *RNA*. 2020:**26**(12):1847–1861. https://doi.org/10.1261/rna.077289.120.

Dostert C, Jouanguy E, Irving P, Troxler L, Galiana-Arnoux D, Hetru C, Hoffmann JA, Imler J-L. The Jak-STAT signaling pathway is required but not sufficient for the antiviral response of Drosophila. *Nat Immunol*. 2005:**6**(9):946–953. https://doi.org/10.1038/ni1237.

Dowel M, Srinivasan A. 2023. data.table: Extension of data.frame. R package version 1.14.8. https://CRAN.R-project.org/package=data.table

Galiana-Arnoux D, Dostert C, Schneemann A, Hoffmann JA, Imler J-L. Essential function in vivo for dicer-2 in host defense against RNA viruses in Drosophila. *Nat Immunol*. 2006:**7**(6):590–597. https://doi.org/10.1038/ni1335.

Gibb R, Redding DW, Chin KQ, Donnelly CA, Blackburn TM, Newbold T, Jones KE. Zoonotic host diversity increases in human-dominated ecosystems. *Nature*. 2020:**584**(7821):398–402. https://doi.org/10.1038/s41586-020-2562-8.

Girardi E, Lefèvre M, Chane-Woon-Ming B, Paro S, Claydon B, Imler J-L, Meignin C, Pfeffer S. Cross-species comparative analysis of dicer proteins during sindbis virus infection. *Sci Rep*. 2015:**5**(1):10693. https://doi.org/10.1038/srep10693.

Gizzi AS, Grove TL, Arnold JJ, Jose J, Jangra RK, Garforth SJ, Du Q, Cahill SM, Dulyaninova NG, Love JD, *et al.* A naturally occurring antiviral ribonucleotide encoded by the human genome. *Nature*. 2018:**558**(7711):610–614. https://doi.org/10.1038/s41586-018-0238-4.

Goodin MM, Hatfull GF, Malik HS. A diversified portfolio. *Annu Rev Virol*. 2016:**3**(1):vi–viii. https://doi.org/10.1146/annurev-vi-3-100316-100011.

Gordon O, Henry CM, Srinivasan N, Ahrens S, Franz A, Deddouche S, Chakravarty P, Phillips D, George R, Kjaer S, *et al.* α-actinin accounts for the bioactivity of actin preparations in inducing STAT target genes in Drosophila melanogaster. *Elife*. 2018:**7**:e38636. https://doi.org/10.7554/eLife.38636.

Goto A, Okado K, Martins N, Cai H, Barbier V, Lamiable O, Troxler L, Santiago E, Kuhn L, Paik D, *et al.* The kinase IKKβ regulates a STING- and NF-κB-dependent antiviral response pathway in Drosophila. *Immunity*. 2018:**49**(2):225–234.e4. https://doi.org/10.1016/j.immuni.2018.07.013.

Graves S, Piepho H, Dorai-Raj LS. 2023. multcompView: Visualizations of Paired Comparisons. R package version 0.1-9. https://CRAN.R-project.org/package=multcompView

Guo Z, Li Y, Ding S-W. Small RNA-based antimicrobial immunity. *Nat Rev Immunol*. 2019:**19**(1):31–44. https://doi.org/10.1038/s41577-018-0071-x.

Hamilton AJ, Baulcombe DC. A species of small antisense RNA in posttranscriptional gene silencing in plants. *Science*. 1999:**286**(5441):950–952. https://doi.org/10.1126/science.286.5441.950.

Holleufer A, Winther KG, Gad HH, Ai X, Chen Y, Li L, Wei Z, Deng H, Liu J, Frederiksen NA, *et al.* Two cGAS-like receptors induce antiviral immunity in Drosophila. *Nature*. 2021:**597**(7874):114–118. https://doi.org/10.1038/s41586-021-03800-z.

Hothorn T, Bretz F, Westfall P. Simultaneous inference in general parametric models. *Biom J*. 2008:**50**(3):346–363. https://doi.org/10.1002/bimj.200810425.

Hua X, Li B, Song L, Hu C, Li X, Wang D, Xiong Y, Zhao P, He H, Xia Q, *et al.* Stimulator of interferon genes (STING) provides insect antiviral immunity by promoting dredd caspase-mediated NF-κB activation. *J. Biol Chem*. 2018:**293**(30):11878–11890. https://doi.org/10.1074/jbc.RA117.000194.

Imler J-L, Cai H, Meignin C, Martins N. Evolutionary immunology to explore original antiviral strategies. Phil. Trans. R. Soc. B. 2024;**379**:20230068. https://doi.org/10.1098/rstb.2023.0068.

Imrie RM, Roberts KE, Longdon B. Between virus correlations in the outcome of infection across host species: evidence of virus by host species interactions. *Evol Lett*. 2021:**5**(5):472–483. https://doi.org/10.1002/evl3.247.

Jactel H, Imler J-L, Lambrechts L, Failloux A-B, Lebreton JD, Maho YL, Duplessy J-C, Cossart P, Grandcolas P. Insect decline: immediate action is needed. *C R Biol*. 2021:**343**(3):267–293. https://doi.org/10.5802/crbiol.37.

Ji Y, Thomas C, Tulin N, Lodhi N, Boamah E, Kolenko V, Tulin AV. Charon mediates immune deficiency–driven PARP-1–dependent immune responses in Drosophila. *J Immunol*. 2016:**197**(6):2382–2389. https://doi.org/10.4049/jimmunol.1600994.

Kassambara A. 2023a. ggpubr: "ggplot2" Based Publication Ready Plots. R package version 0.6.0. https://CRAN.R-project.org/package=ggpubr

Kassambara A. 2023b. rstatix: Pipe-Friendly Framework for Basic Statistical Tests. R package version 0.7.2. https://CRAN.R-project.org/package=rstatix

Kassambara A, Kosinski M, Biecek P. 2021. survminer: Drawing Survival Curves using "ggplot2". R package version 0.4.9. https://CRAN.R-project.org/package=survminer

Kawai T, Akira S. Toll-like receptors and their crosstalk with other innate receptors in infection and immunity. *Immunity*. 2011:**34**(5):637–650. https://doi.org/10.1016/j.immuni.2011.05.006.

Kemp C, Mueller S, Goto A, Barbier V, Paro S, Bonnay F, Dostert C, Troxler L, Hetru C, Meignin C, *et al.* Broad RNA interference-mediated antiviral immunity and virus-specific inducible responses in Drosophila. *J Immunol*. 2013:**190**(2):650–658. https://doi.org/10.4049/jimmunol.1102486.

Kim D, Langmead B, Salzberg SL. HISAT: a fast spliced aligner with low memory requirements. *Nat Methods*. 2015:**12**(4):357–360. https://doi.org/10.1038/nmeth.3317.

Lafont M, Vergnes A, Vidal-Dupiol J, de Lorgeril J, Gueguen Y, Haffner P, Petton B, Chaparro C, Barrachina C, Destoumieux-Garzon D, *et al.* A sustained immune response supports long-term antiviral immune priming in the pacific oyster, crassostrea gigas. *mBio*. 2020:**11**(2):e02777-19. https://doi.org/10.1128/mBio.02777-19.

Lamiable O, Kellenberger C, Kemp C, Troxler L, Pelte N, Boutros M, Marques JT, Daeffler L, Hoffmann JA, Roussel A, *et al.* Cytokine diedel and a viral homologue suppress the IMD pathway in Drosophila. *Proc Natl Acad Sci U S A*. 2016:**113**(3):698–703. https://doi.org/10.1073/pnas.1516122113.

Lažetić V, Batachari LE, Russell AB, Troemel ER. Similarities in the induction of the intracellular pathogen response in caenorhabditis elegans and the type I interferon response in mammals. *BioEssays*. 2023:**45**(11):2300097. https://doi.org/10.1002/bies.202300097.

Lenth R. 2023. emmeans: Estimated Marginal Means, aka Least-Squares Means. R package version 1.8.8. https://CRAN.R-project.org/package=emmeans

Lewandowska M, Sharoni T, Admoni Y, Aharoni R, Moran Y. Functional characterization of the cnidarian antiviral immune response reveals ancestral complexity. *Mol Biol Evol*. 2021:**38**(10):4546–4561. https://doi.org/10.1093/molbev/msab197.

Li Y, Slavik KM, Toyoda HC, Morehouse BR, de Oliveira Mann CC, Elek A, Levy S, Wang Z, Mears KS, Liu J, *et al.* cGLRs are a diverse family of pattern recognition receptors in innate immunity. *Cell*. 2023:**186**(15):3261–3276.e20. https://doi.org/10.1016/j.cell.2023.05.038.

Liao Y, Smyth GK, Shi W. featureCounts: an efficient general purpose program for assigning sequence reads to genomic features. *Bioinformatics*. 2014:**30**(7):923–930. https://doi.org/10.1093/bioinformatics/btt656.

Liu Y, Gordesky-Gold B, Leney-Greene M, Weinbren NL, Tudor M, Cherry S. Inflammation-Induced, STING-dependent autophagy restricts Zika virus infection in the Drosophila brain. *Cell Host Microbe*. 2018:**24**(1):57–68.e3. https://doi.org/10.1016/j.chom.2018.05.022.

Liu Q, Yi D, Ding J, Mao Y, Wang S, Ma L, Li Q, Wang J, Zhang Y, Zhao J, *et al.* MOV10 recruits DCP2 to decap human LINE-1 RNA by forming large cytoplasmic granules with phase separation properties. *EMBO Rep*. 2023:**24**(9):e56512. https://doi.org/10.15252/embr.202256512.

Longdon B, Hadfield JD, Day JP, Smith SCL, McGonigle JE, Cogni R, Cao C, Jiggins FM. The causes and consequences of changes in virulence following pathogen host shifts. *PLoS Pathog*. 2015:**11**(3):e1004728. https://doi.org/10.1371/journal.ppat.1004728.

Love MI, Huber W, Anders S. Moderated estimation of fold change and dispersion for RNA-Seq data with DESeq2. *Genome Biol*. 2014:**15**(12):550. https://doi.org/10.1186/s13059-014-0550-8.

Lu R, Maduro M, Li F, Li HW, Broitman-Maduro G, Li WX, Ding SW. Animal virus replication and RNAi-mediated antiviral silencing in *Caenorhabditis elegans*. *Nature*. 2005:**436**(7053):1040–1043. https://doi.org/10.1038/nature03870.

Lüdecke D, Waggoner PD, Makowski D. Insight: a unified interface to access information from model objects in R. *J Open Source Softw*. 2019:**4**(38):1412. https://doi.org/10.21105/joss.01412.

Magwire MM, Fabian DK, Schweyen H, Cao C, Longdon B, Bayer F, Jiggins FM. Genome-wide association studies reveal a simple genetic basis of resistance to naturally coevolving viruses in

Drosophila melanogaster. *PLoS Genet*. 2012:**8**(11):e1003057. https://doi.org/10.1371/journal.pgen.1003057.
Maillard PV, Van der Veen AG, Deddouche-Grass S, Rogers NC, Merits A, Reis e Sousa C. Inactivation of the type I interferon pathway reveals long double-stranded RNA-mediated RNA interference in mammalian cells. *EMBO J*. 2016:**35**(23): 2505–2518. https://doi.org/10.15252/embj.201695086.
Margolis SR, Dietzen PA, Hayes BM, Wilson SC, Remick BC, Chou S, Vance RE. The cyclic dinucleotide 2′3′-cGAMP induces a broad antibacterial and antiviral response in the sea anemone Nematostella vectensis. *Proc Natl Acad Sci U S A*. 2021:**118**(51). https://doi.org/10.1073/pnas.2109022118.
Marques JT, Wang J-P, Wang X, de Oliveira KPV, Gao C, Aguiar ERGR, Jafari N, Carthew RW. Functional specialization of the small interfering RNA pathway in response to virus infection. *PLoS Pathog*. 2013:**9**(8):e1003579. https://doi.org/10.1371/journal.ppat.1003579.
Martin M, Hiroyasu A, Guzman RM, Roberts SA, Goodman AG. Analysis of Drosophila STING reveals an evolutionarily conserved antimicrobial function. *Cell Rep*. 2018:**23**(12):3537–3550.e6. https://doi.org/10.1016/j.celrep.2018.05.029.
Martins NE, Faria VG, Nolte V, Schlötterer C, Teixeira L, Sucena É, Magalhães S. Host adaptation to viruses relies on few genes with different cross-resistance properties. *Proc Natl Acad Sci U S A*. 2014:**111**(16):5938–5943. https://doi.org/10.1073/pnas.1400378111.
McDougal MB, Boys IN, De La Cruz-Rivera P, Schoggins JW. Evolution of the interferon response: lessons from ISGs of diverse mammals. *Curr Opin Virol*. 2022:**53**:101202. https://doi.org/10.1016/j.coviro.2022.101202.
Medzhitov R, Schneider DS, Soares MP. Disease tolerance as a defense strategy. *Science*. 2012:**335**(6071):936–941. https://doi.org/10.1126/science.1214935.
Merkling SH, Bronkhorst AW, Kramer JM, Overheul GJ, Schenck A, Van Rij RP. The epigenetic regulator G9a mediates tolerance to RNA virus infection in Drosophila. *PLoS Pathog*. 2015a:**11**(4):e1004692. https://doi.org/10.1371/journal.ppat.1004692.
Merkling SH, Overheul GJ, van Mierlo JT, Arends D, Gilissen C, van Rij RP. The heat shock response restricts virus infection in Drosophila. *Sci Rep*. 2015b:**5**(1):12758. https://doi.org/10.1038/srep12758.
Mondotte JA, Gausson V, Frangeul L, Blanc H, Lambrechts L, Saleh M-C. Immune priming and clearance of orally acquired RNA viruses in Drosophila. *Nat Microbiol*. 2018:**3**(12):1394–1403. https://doi.org/10.1038/s41564-018-0265-9.
Morris O, Liu X, Domingues C, Runchel C, Chai A, Basith S, Tenev T, Chen H, Choi S, Pennetta G, *et al*. Signal integration by the IκB protein pickle shapes Drosophila innate host defense. *Cell Host Microbe*. 2016:**20**(3):283–295. https://doi.org/10.1016/j.chom.2016.08.003.
Obbard DJ, Maclennan J, Kim K-W, Rambaut A, O'Grady PM, Jiggins FM. Estimating divergence dates and substitution rates in the Drosophila phylogeny. *Mol Biol Evol*. 2012:**29**(11):3459–3473. https://doi.org/10.1093/molbev/mss150.
Olmo RP, Ferreira AGA, Izidoro-Toledo TC, Aguiar ERGR, de Faria IJS, de Souza KPR, Osório KP, Kuhn L, Hammann P, de Andrade EG, *et al*. Control of dengue virus in the midgut of aedes aegypti by ectopic expression of the dsRNA-binding protein loqs2. *Nat Microbiol*. 2018:**3**(12):1385–1393. https://doi.org/10.1038/s41564-018-0268-6.
Ooms J, McNamara J. 2023. Export Data Frames to Excel "xlsx" Format. R package version 1.4.2. https://CRAN.R-project.org/package=writexl
Panda D, Pascual-Garcia P, Dunagin M, Tudor M, Hopkins KC, Xu J, Gold B, Raj A, Capelson M, Cherry S. Nup98 promotes antiviral gene expression to restrict RNA viral infection in Drosophila. *Proc Natl Acad Sci U S A*. 2014:**111**(37):E3890–E3899. https://doi.org/10.1073/pnas.1410087111.
Paradis E, Schliep K. Ape 5.0: an environment for modern phylogenetics and evolutionary analyses in R. *Bioinformatics*. 2019: **35**(3):526–528. https://doi.org/10.1093/bioinformatics/bty633.
Pennell MW, Eastman JM, Slater GJ, Brown JW, Uyeda JC, FitzJohn RG, Alfaro ME, Harmon LJ. . Geiger v2.0: an expanded suite of methods for fitting macroevolutionary models to phylogenetic trees. *Bioinformatics*. 2014:**30**(15):2216–2218. https://doi.org/10.1093/bioinformatics/btu181.
Pichlmair A, Lassnig C, Eberle C-A, Górna MW, Baumann CL, Burkard TR, Bürckstümmer T, Stefanovic A, Krieger S, Bennett KL, *et al*. IFIT1 is an antiviral protein that recognizes 5′-triphosphate RNA. *Nat Immunol*. 2011:**12**(7):624–630. https://doi.org/10.1038/ni.2048.
Pinheiro J, Bates D, R Core Team. 2023 . nlme: Linear and Nonlinear Mixed Effects Models. R package version 3.1-163. https://CRAN.R-project.org/package=nlme
Plummer M, Best N, Cowles K, Vines K. CODA: convergence diagnosis and output analysis for MCMC. *R News*. 2006:**6**(1):7–11. https://cran.r-project.org/doc/Rnews/Rnews_2006-1.pdf.
Plus N, Croizier G, Reinganum C, Scott PD. Cricket paralysis virus and Drosophila C virus: serological analysis and comparison of capsid polypeptides and host range. *J Invertebr Pathol*. 1978:**31**(3): 296–302. https://doi.org/10.1016/0022-2011(78)90219-7.
Poirier EZ, Buck MD, Chakravarty P, Carvalho J, Frederico B, Cardoso A, Healy L, Ulferts R, Beale R, Reis e E, *et al*. An isoform of dicer protects mammalian stem cells against multiple RNA viruses. *Science*. 2021:**373**(6551):231–236. https://doi.org/10.1126/science.abg2264.
Posit team. *RStudio: integrated development environment for R*. Boston (MA): Posit Software, PBC; 2023.
Ratcliff F, Harrison BD, Baulcombe DC. A similarity between viral defense and gene silencing in plants. *Science*. 1997:**276**(5318): 1558–1560. https://doi.org/10.1126/science.276.5318.1558.
R Core Team. *R: A language and environment for statistical computing*. Vienna, Austria: R Foundation for Statistical Computing; 2023.
Revell L. Phytools: an R package for phylogenetic comparative biology (and other things). *Methods Ecol Evol*. 2012:**3**(2):217–223. https://doi.org/10.1111/j.2041-210X.2011.00169.x.
Roberts KE, Longdon B. Viral susceptibility across host species is largely independent of dietary protein to carbohydrate ratios. *J Evol Biol*. 2021:**34**(5):746–756. https://doi.org/10.1111/jeb.13773.
Roers A, Hiller B, Hornung V. Recognition of endogenous nucleic acids by the innate immune system. *Immunity*. 2016:**44**(4): 739–754. https://doi.org/10.1016/j.immuni.2016.04.002.
Rutschmann S, Jung AC, Zhou R, Silverman N, Hoffmann JA, Ferrandon D. Role of Drosophila IKK gamma in a toll-independent antibacterial immune response. *Nat Immunol*. 2000:**1**(4):342–347. https://doi.org/10.1038/79801.
Sabatier L, Jouanguy E, Dostert C, Zachary D, Dimarcq J-L, Bulet P, Imler J-L. Pherokine-2 and -3. *Eur J Biochem*. 2003:**270**(16): 3398–3407. https://doi.org/10.1046/j.1432-1033.2003.03725.x.
Sansone CL, Cohen J, Yasunaga A, Xu J, Osborn G, Subramanian H, Gold B, Buchon N, Cherry S. Microbiota-Dependent priming of antiviral intestinal immunity in Drosophila. *Cell Host Microbe*. 2015:**18**(5):571–581. https://doi.org/10.1016/j.chom.2015.10.010.
Schneider WM, Chevillotte MD, Rice CM. Interferon-stimulated genes: a complex web of host defenses. *Annu Rev Immunol*. 2014:**32**(1):513–545. https://doi.org/10.1146/annurev-immunol-032713-120231.
Schoggins JW. Interferon-Stimulated genes: what do they all do? *Annu Rev Virol*. 2019:**6**(1):567–584. https://doi.org/10.1146/annurev-virology-092818-015756.
Schoggins JW, MacDuff DA, Imanaka N, Gainey MD, Shrestha B, Eitson JL, Mar KB, Richardson RB, Ratushny AV, Litvak V, *et al*. Pan-viral specificity of IFN-induced genes reveals new roles for cGAS in innate immunity. *Nature*. 2014:**505**(7485):691–695. https://doi.org/10.1038/nature12862.
Schoggins JW, Wilson SJ, Panis M, Murphy MY, Jones CT, Bieniasz P, Rice CM. A diverse range of gene products are effectors of the

type I interferon antiviral response. *Nature*. 2011:**472**(7344): 481–485. https://doi.org/10.1038/nature09907.

Segrist E, Dittmar M, Gold B, Cherry S. Orally acquired cyclic dinucleotides drive dSTING-dependent antiviral immunity in enterocytes. *Cell Rep*. 2021:**37**(13):110150. https://doi.org/10.1016/j.celrep.2021.110150.

Shaw AE, Hughes J, Gu Q, Behdenna A, Singer JB, Dennis T, Orton RJ, Varela M, Gifford RJ, Wilson SJ, *et al.* Fundamental properties of the mammalian innate immune system revealed by multispecies comparison of type I interferon responses. *PLoS Biol*. 2017:**15**(12): e2004086. https://doi.org/10.1371/journal.pbio.2004086.

Slavik KM, Morehouse BR, Ragucci AE, Zhou W, Ai X, Chen Y, Li L, Wei Z, Bähre H, König M, *et al.* cGAS-like receptors sense RNA and control 3′2′-cGAMP signalling in Drosophila. *Nature*. 2021:**597**(7874): 109–113. https://doi.org/10.1038/s41586-021-03743-5.

Souza-Neto JA, Sim S, Dimopoulos G. An evolutionary conserved function of the JAK-STAT pathway in anti-dengue defense. *Proc Natl Acad Sci U S A*. 2009:**106**(42):17841–17846. https://doi.org/10.1073/pnas.0905006106.

Swevers L, Liu J, Smagghe G. Defense mechanisms against viral infection in Drosophila: rNAi and non-RNAi. *Viruses*. 2018:**10**(5):230. https://doi.org/10.3390/v10050230.

Tenthorey JL, Emerman M, Malik HS. Evolutionary landscapes of host-virus arms races. *Annu Rev Immunol*. 2022:**40**:271–294. https://doi.org/10.1146/annurev-immunol-072621-084422.

Therneau TM. 2022. coxme: Mixed Effects Cox Models. R package version 2.2-18.1. https://CRAN.R-project.org/package=coxme.

Therneau T. 2023. A Package for Survival Analysis in R. R package version 3.5-7. https://CRAN.R-project.org/package=survival

Thiébaut A, Altenhoff AM, Campli G, Glover N, Dessimoz C, Waterhouse RM. 2023. DrosOMA: the *Drosophila* Orthologous Matrix browser. https://f1000research.com/articles/12-936

van Rij RP, Saleh M-C, Berry B, Foo C, Houk A, Antoniewski C, AndinoR. The RNA silencing endonuclease argonaute 2 mediates specific antiviral immunity in Drosophila melanogaster. *Genes Dev*. 2006:**20**(21):2985–2995. https://doi.org/10.1101/gad.1482006.

Veen AG, Maillard PV, Schmidt JM, Lee SA, Deddouche-Grass S, Borg A, Kjær S, Snijders AP, Reis e Sousa C. The RIG-I-like receptor LGP2 inhibits dicer-dependent processing of long double-stranded RNA and blocks RNA interference in mammalian cells. *EMBO J*. 2018:**37**(4):e97479. https://doi.org/10.15252/embj.201797479.

Wang X-H, Aliyari R, Li W-X, Li H-W, Kim K, Carthew R, Atkinson P, Ding S-W. RNA interference directs innate immunity against viruses in adult Drosophila. *Science*. 2006:**312**(5772):452–454. https://doi.org/10.1126/science.1125694.

Wickham H. *Ggplot2: elegant graphics for data analysis*. 2nd ed. Springer International Publishing; 2016. https://doi.org/10.1007/978-3-319-24277-4.

Wickham H. 2022. stringr: Simple, Consistent Wrappers for Common String Operations. R package version 1.5.0. https://CRAN.R-project.org/package=stringr.

Wickham H, Averick M, Bryan J, Chang W, McGowan LDA, François R, Grolemund G, Hayes A, Henry LA, Hester JJ, *et al.* Welcome to the tidyverse. *J Open Source Softw*. 2019:**4**:1686. https://doi.org/10.21105/joss.01686.

Wickham H, Bryan J. 2023. readxl: Read Excel Files. R package version 1.4.3. https://CRAN.R-project.org/package=readxl

Wickham H, François R, Henry L, Müller K, Vaughan D. 2023. dplyr: A Grammar of Data Manipulation. R package version 1.1.2. https://dplyr.tidyverse.org, https://github.com/tidyverse/dplyr.

Wickham H, Henry L. 2023. purrr: Functional Programming Tools. R package version 1.0.1. https://CRAN.R-project.org/package=purrr

Wickham H, Seidel D. 2022. scales: Scale Functions for Visualization. R package version 1.2.1. https://CRAN.R-project.org/package=scales

Williams BR. PKR; a sentinel kinase for cellular stress. *Oncogene*. 1999:**18**(45):6112–6120. https://doi.org/10.1038/sj.onc.1203127.

Woznica A, Kumar A, Sturge CR, Xing C, King N, Pfeiffer JK. STING mediates immune responses in the closest living relatives of animals. *eLife*. 2021:**10**:e70436. https://doi.org/10.7554/eLife.70436.

Wu J, Sun L, Chen X, Du F, Shi H, Chen C, Chen ZJ. Cyclic GMP-AMP is an endogenous second messenger in innate immune signaling by cytosolic DNA. *Science*. 2013:**339**(6121):826–830. https://doi.org/10.1126/science.1229963.

Wu X, Wu F-H, Wang X, Wang L, Siedow JN, Zhang W, Pei Z-M. 2014. Molecular evolutionary and structural analysis of the cytosolic DNA sensor cGAS and STING. *Nucleic Acids Res*. **42**(13): 8243–8257. https://doi.org/10.1093/nar/gku569.

Xie Y. 2023. tinytex: Helper Functions to Install and Maintain TeX Live, and Compile LaTeX Documents. R package version 0.46. https://github.com/rstudio/tinytex

Xu J, Grant G, Sabin LR, Gordesky-Gold B, Yasunaga A, Tudor M, Cherry S. Transcriptional pausing controls a rapid antiviral innate immune response in Drosophila. *Cell Host Microbe*. 2012:**12**(4): 531–543. https://doi.org/10.1016/j.chom.2012.08.011.

Zhu H. 2021. kableExtra: Construct Complex Table with "kable" and Pipe Syntax. R package version 1.3.4. https://CRAN.R-project.org/package=kableExtra